An Exact Dynamic Stiffness Method for Multibody Systems Consisting of Beams and Rigid-Bodies

Xiang Liu[1], Chengli Sun[2], J. Ranjan Banerjee[3], Han-Cheng Dan[4]*, Le Chang[5]

1. **Xiang Liu**, Professor, Ph.D., Key Laboratory of Traffic Safety on Track, Ministry of Education, School of Traffic & Transportation Engineering, Central South University, Changsha, China; Joint International Research Laboratory of Key Technology for Rail Traffic Safety, Central South University, Changsha, China; State Key Laboratory of High Performance Complex Manufacturing, Central South University, Changsha, China; Email: xiangliu06@gmail.com
2. **Chengli Sun**, Postgraduate, Key Laboratory of Traffic Safety on Track, Ministry of Education, School of Traffic & Transportation Engineering, Central South University, Changsha, China; Joint International Research Laboratory of Key Technology for Rail Traffic Safety, Central South University, Changsha, China; Email: 1454744546@qq.com
3. **J. Ranjan Banerjee**, Professor, DSc., School of Mathematics, Computer Science and Engineering, City University London, London EC1V 0HB, UK; Email: j.r.banerjee@city.ac.uk
4. **Han-Cheng Dan**, Associate Professor, Ph.D., School of Civil Engineering, Central South University, Changsha, China; Email: danhancheng@csu.edu.cn
5. **Le Chang**, Postgraduate, Key Laboratory of Traffic Safety on Track, Ministry of Education, School of Traffic & Transportation Engineering, Central South University, Changsha, China; Joint International Research Laboratory of Key Technology for Rail Traffic Safety, Central South University, Changsha, China; Email: 1078877539@qq.com

*Corresponding author: Dan Han-Cheng, Email: danhancheng@csu.edu.cn

Abstract: An exact dynamic stiffness method is proposed for the free vibration analysis of multi-body systems consisting of flexible beams and rigid bodies. The theory is sufficiently general in that the rigid bodies can be of any shape or size, but importantly, the theory permits connections of the rigid bodies to any number beams at any arbitrary points and oriented at any arbitrary angles. For beam members, a range of theories including the Bernoulli-Euler and Timoshenko theories are applied. The assembly procedure for the beam and rigid body properties is simplified without resorting to matrix inversion. The difficulty generally encountered in computing the problematic J_0 count when applying the Wittrick-Williams algorithm for modal analysis has been overcome. Applications of different beam theories for both axial and bending vibrations have enabled the examination of the role played by rigid-body parameters on the multi-body system's dynamic behaviour. Some exact benchmark results are provided and compared with published results and with finite element solutions. This research provides an exact and highly efficient analysis tool for multibody system dynamics which is for the free vibration analysis, ideally suited for optimization and inverse problems such as modal parameter identification.

Keywords: Multibody system; Dynamic stiffness method; Wittrick-Williams algorithm; Exact modal analysis; Rigid body; Rayleigh-Love theory and Timoshenko theory.

1 Introduction

Multi-body system is a system in which a certain number of rigid and deformable bodies are connected together in some prearranged way[1,2]. The applications of multi-body systems are wide ranging which include military, aerospace, rail transportation, satellite launch systems, aircraft, spacecraft, cars, trains, robotics, amongst many other areas of engineering. The dynamic behaviour of multi-body systems plays a vital, if not crucial role in their design. It is well known that different types of attachments for flexible and rigid parts of a multibody system can affect the overall dynamic behaviour of the combined system significantly. In this respect, many theories have been proposed in recent years to deal with multi-body systems, particularly those consisting of beams and rigid bodies [3–6]. Based on the literature review carried out by the authors, the published research in the area can be broadly classified in two groups, of which one relies on numerical methods whereas the other focuses on analytical methods. The advantages and disadvantages of these two approaches have been outlined in the literature [1,2].

From a numerical perspective, one of the commonly used commercial software ANSYS provides an option to model a beam and rigid-body connection when representing a built-up structure, but the application of this kind of software for multibody system is not always reliable or effective. This is because numerical instabilities might occur when using such software due to marked differences in the mass and stiffness properties of rigid and deformable bodies, particularly when higher natural frequencies are of interest. This has inspired researchers to explore various alternative routes using both numerical and non-numerical methods. For instance, Yoo et al.[2] used a computer simulation method to demonstrate the validity of the absolute node coordinate formula (ANCF) on large displacement and large deformation problems. The authors showed that their method can be applied to practical multi-body systems, as encountered in engineering problems. Many other simulation models [7,8] have also been proposed to address significant practical engineering problems involving multibody systems. Evidently the existing research in many ways, proved that numerical methods can be suitably adapted to dynamic analysis of various multi-body systems. Wu[9] presented an elastic-and-rigid-combined beam element model, in which the finite element method was basically used. In a follow up paper, Wu[10] proposed an improved finite element method of rigid bars supported by several elastic beams. On the above numerical models, dynamic analysis was performed by using well-established numerical solvers which can be applied to a wide range of problems. However, in most of the above numerical methods, the beam members have been discretized into elements that are represented by approximate shape functions and the modelling process requires many elements to idealise a realistic structure and achieve acceptable accuracy. This inevitably incurs lot of computational efforts and may introduce inaccuracies, particularly when computing higher natural frequencies and mode shapes. Therefore, methods predominantly based on numerical techniques are not always suitable for modal analysis in the high frequency range[11].

To circumvent the above problem, many analytical models have been proposed for beam structures connected to various types of attachments such as lumped concentrated mass [12–16] and/or rotatory inertia [17], spring and damper [18], single spring-mass [14,19–26], double spring-mass[27–32], spring-mass chain[33,34] which all have wide ranging applications in engineering. The attachment as lumped mass used in these publications is by and large assumed to be a concentrated point mass without any consideration to the size or dimension of the mass or its mass moment of inertia. It was therefore, much easier for these earlier investigators to realise an analytical model of a multibody system using such a simplistic approach. Of course, for the problems with attachments represented by two or more degrees of freedom together with the consideration of their physical dimensions, the analytical formulation will be much more complex, see for example the attachment of a two-degree-of-freedom systems [35–37], mass-spring-mass-damper [38] and two-part beam-mass [39–47]. It should be recognised at this stage that one of the accurate and popular methods of modelling a multi-body system is the transfer matrix method [29,46,48–50], which is relatively simple to use and is seemingly efficient, particularly when analysing chain-like multi-body systems. However, the method can become complicated and even unimplementable for branch-like multi-body systems. One of the downsides of the transfer matrix method is that numerical errors can easily build up and accumulate during the successive matrix manipulation process which may, of course may lead to numerical ill-conditioning or inaccuracy in results. It is evident from the existing literature that the flexible beam members used in modelling multibody systems are mainly based on classical Euler-Bernoulli theory when dealing with bending and axial vibration problems [51]. This is rather restrictive because the theory is suitable only for slender beam members, but not for thicker or shorter ones. For short and thick beam members which are often encountered in engineering applications, more advanced theories are needed, e.g. Timoshenko theory [52–54] which considers the effects of shear deformation and rotatory inertia in bending vibration and Rayleigh-Love theory [54] which accounts for transverse inertia in axial vibration. The importance of applying the Timoshenko theory to model beam members in multibody systems has recently been emphasised by some authors [15,34,47,55], although apparently not much attention has been paid on the effects of considering advanced beam theories in the multibody dynamics. However, it has to be mentioned in passing that there are well-developed dynamic stiffness theories for beam elements in the literature[36,52–54,56–60] which are relevant and can be helpful in this context.

Although different analytical models have been proposed for multibody systems, unfortunately, they are not all sufficiently well-equipped with efficient, accurate and robust solution techniques which are really necessary. Thus, there are some difficulties to apply these existing methods to complex multibody systems. For example, unlike the numerical method where the stiffness and mass matrices can be formulated separately [9], almost all existing analytical methods [45–50,2,6,13,52,14,15,22–24,26,27,29–31,55,32–35,37–40,42,44,61,62] apply the usual determinant method for non-trivial solution of the eigenvalue problem for which the determinant of the coefficient matrix vanishes. The determinant method needs the evaluation of the determinant numerically for one

frequency at a time. Deciding the step size to find the zeroes of the frequency-determinant and avoid the poles is far from being trivial. The problem arises because a small step size leads to unnecessary computational cost whereas a large step size increases the possibility of missing some genuine natural frequencies. This is especially true for complex structures and when computing higher order natural frequencies. The problem is further compounded by the fact that the frequency determinant often involves complex and irregular transcendental functions such as the hyperbolic functions. Some efforts have been made in the literature to convert the zero-finding procedure to an optimisation problem[49] and also to reduce the matrix size [37] when solving the eigenvalue problem. Nevertheless, the potential pitfalls and drawbacks of the determinant method as mentioned above, still exist. Furthermore, extra efforts are needed to compute the mode shapes and also to apply general boundary conditions[9]. Against this background, there is an accurate, efficient and robust solution technique, called the Wittrick-Williams algorithm [19], which extracts eigenvalues with certainty from analytical dynamic stiffness formulations. This powerful algorithm has been utilized previously with great success when solving free vibration problems of plane frames[53,54,56] and with attachments such as concentrated mass, spring mass[57] and two-degree-of-freedom system[36]. However, the application of the Wittrick-Williams algorithm may encounter some difficulty in solving complex multibody system such as a two-part beam-mass system [41,57] where the so-called J_0 count of the condensed system is not readily available.

The main purpose of this paper is to propose an accurate, efficient, reliable and versatile analytical method for the free vibration analysis of multibody systems involving rigid bodies coupled with beam elements, for the most general case. The proposed method has the following attributes and novel features: 1) The formulation is versatile because any number of rigid bodies can be connected to any number of beam members at any arbitrary points and at any arbitrary angles. 2) The assembly procedure is straightforward to make the method easy to implement in a computer program and thus, suitable for modelling complex beam-rigid body built-up structures (there is no restriction on the theories to be applied for beam members), 3) The formulation does not cause extra difficulties to the solution technique based on the Wittrick-Williams algorithm, particularly the J_0 count problem, ensuring the solution technique to be both efficient and robust. 4) Both the formulation and solution technique do not involve matrix inversion or determinant evaluation and hence, avoid introducing any undesirable numerical instability or inaccuracy. This research provides the basis of a general framework for modelling complex multibody structures in engineering installation by using an exact analytical dynamic stiffness formulation. The proposed method is ideally suited for optimization and inverse problems [63–65] such as modal parameter identification.

The paper is organized as follows. Following this Introduction, Section 2 highlights the application ranges of the theory, the analytical formulation, assembly procedure and the solution technique. Then, Section 3 validates the proposed method and demonstrates its wide application range through some illustrative practical

engineering applications. Finally, Section 4 concludes the paper. The Appendix briefly summarizes the dynamic stiffness formulations of different types of beam elements.

2 Theory

This section describes the exact dynamic stiffness formulation of a multi-body system consisting of flexible beams and rigid bodies. The model is sufficiently general in which the rigid bodies can be of any shape and size and they can be connected to any number of flexible beams at any number of arbitrary points with the orientation of any arbitrary angles. The multi-body system studied here is shown in **Fig. 1**, where the line segments represent beam elements, which can undergo both axial and bending deformations. The axial vibration can be described either by classical theory or by Rayleigh-Love theory; whereas the bending vibration is governed by the Bernoulli-Euler theory or by the Timoshenko theory. The dynamic stiffness formulations for the above four theories [51,53,54,66] have been developed by previous researchers , which lead to four possible combinations of the application of these theories when interfaced with rigid-body dynamics. For illustrative purposes, the shaded areas in 错误!未找到引用源。 **1** represent rigid bodies, whose physical characteristics are represented by mass and mass moment of inertia [48].

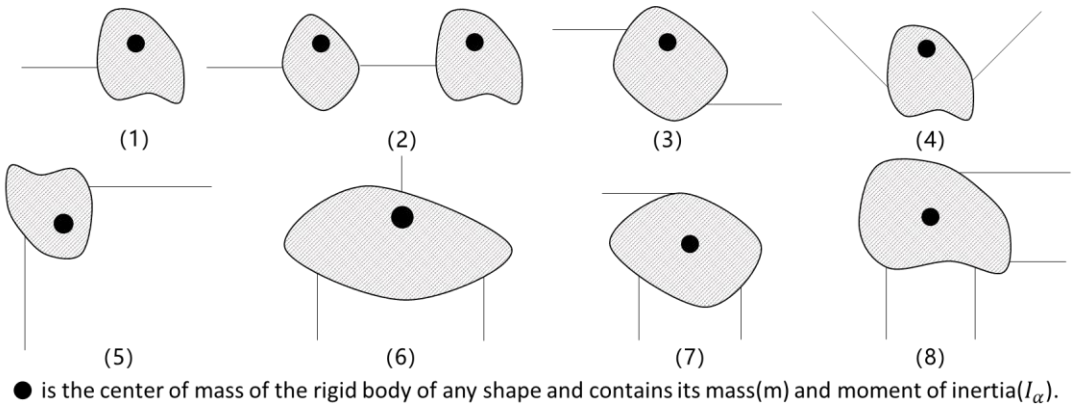

Fig. 1. Schematic diagrams for different ways that rigid bodies are connected to any number of flexible beams at arbitrary points with any arbitrary angles.

In order to demonstrate the dynamic stiffness formulation procedure, we adopt for convenience a multi-body system with one rigid body element ④ connecting three flexible beam elements (①, ② and ③) at points (nodes) 2, 4 and 6 respectively, as shown in **Fig. 2**. First, the dynamic stiffness matrices of the three beam members are formulated from the governing differential equations based on a choice of the different beam theories given in the Appendix. Then, the geometrical and equilibrium relationships of the rigid body and each beam member are formulated using a matrix transformation process, and the dynamic stiffness matrix of each beam member is transformed where the beam node connecting to the rigid body is shifted to the mass centre of the rigid body (this procedure has been performed here for the three elements connecting 3-1, 1-5 and 1-7 segments, only for convenience, but the theory is sufficiently general so that segments can be added). Finally, the overall dynamic

stiffness matrix of the multi-body system is assembled directly from the adjacent node 1, and by applying the corresponding boundary conditions.

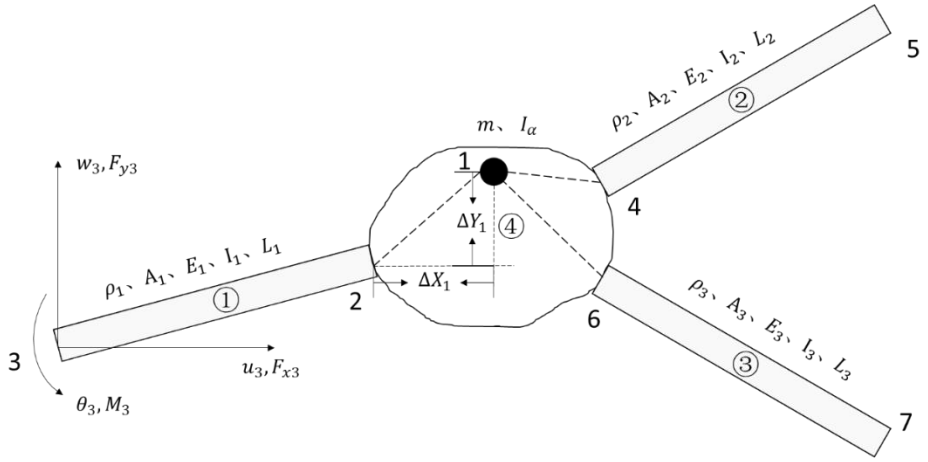

Fig. 2. The rigid body ④ is connected to three beam elements (①, ② and ③) at nodes 2, 4 and 6, respectively.

In order to help the readers, understand the steps used in the proposed method, a flow chart demonstrating the dynamic stiffness modelling procedure for a multibody system is shown in Fig. 3.

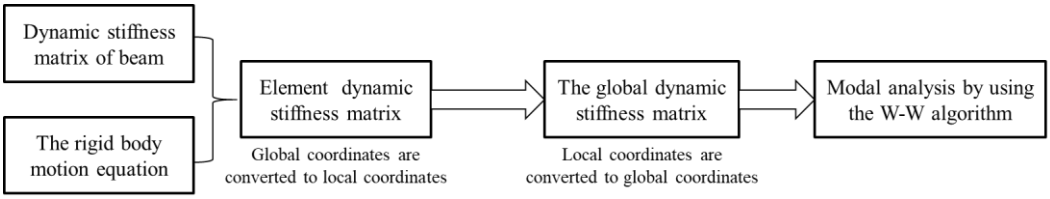

Fig. 3. Dynamic stiffness modelling procedure for a multibody system

2.1 Dynamic stiffness matrix of a beam

The dynamic stiffness (DS) formulations for free vibration of plane frames incorporating the axial and bending deformations have already been developed by many authors based on different theories. For example, the DS formulations for axial vibration of a beam member based on different theories such as classical theory[51], Rayleigh-Love theory[54], Rayleigh-Bishop theory[54] are readily available in the literature. The DS formulations for bending vibration include, but not limited to the Bernoulli-Euler theory [51], the Timoshenko theory[54] and the higher-order shear deformation theory [58]. For beam members with more complex cross-sections and/or made of composite materials, the axial vibration and bending vibration may be coupled due to the fibrous nature of anisotropic composites. For all these beam theories, the dynamic stiffness matrix can be written in the following general form.

$$\begin{bmatrix} F_{x1} \\ F_{y1} \\ M_1 \\ F_{x2} \\ F_{y2} \\ M_2 \end{bmatrix} = \begin{bmatrix} k_{11} & k_{12} & k_{13} & k_{14} & k_{15} & k_{16} \\ k_{21} & k_{22} & k_{23} & k_{24} & k_{25} & k_{26} \\ k_{31} & k_{32} & k_{33} & k_{34} & k_{35} & k_{36} \\ k_{41} & k_{42} & k_{43} & k_{44} & k_{45} & k_{46} \\ k_{51} & k_{52} & k_{53} & k_{54} & k_{55} & k_{56} \\ k_{61} & k_{62} & k_{63} & k_{64} & k_{65} & k_{66} \end{bmatrix} \begin{bmatrix} u_1 \\ w_1 \\ \theta_1 \\ u_2 \\ w_2 \\ \theta_2 \end{bmatrix} \quad (1)$$

where F_x, F_y and M with suffices 1 and 2 represent the axial force, shear force, and bending moment at the two end nodes (1 and 2) of the beam member, respectively; u, w and θ with suffices 1 and 2 represent amplitudes of the axial displacement, the vertical or bending displacement, and the angular or bending rotation of the beam cross-section at the two end nodes of the beam member, respectively. Note that the 6×6 stiffness matrix shown in Eq. (1) must be symmetric.

Although the theory proposed in this paper is general so that it can be applied to any type of beam element considering both axial and bending vibrations [67], for demonstration purposes, we adopt here, the case when the axial vibration and bending vibration of the beam are uncoupled in local coordinates. For clarity and completeness and importantly to make the paper self-contained, analytical expressions [36,51,54,56] for the dynamic stiffness coefficients of the beams under consideration are provided in the Appendix. The element dynamic stiffness matrix of Eq.(1) takes the following form for the uncoupled case.

$$\begin{bmatrix} F_{x1} \\ F_{y1} \\ M_1 \\ F_{x2} \\ F_{y2} \\ M_2 \end{bmatrix} = \begin{bmatrix} a_1 & 0 & 0 & a_2 & 0 & 0 \\ 0 & d_1 & d_2 & 0 & d_4 & -d_5 \\ 0 & d_2 & d_3 & 0 & -d_5 & d_6 \\ a_2 & 0 & 0 & a_1 & 0 & 0 \\ 0 & d_4 & -d_5 & 0 & d_1 & -d_2 \\ 0 & -d_5 & d_6 & 0 & -d_2 & d_3 \end{bmatrix} \begin{bmatrix} u_1 \\ w_1 \\ \theta_1 \\ u_2 \\ w_2 \\ \theta_2 \end{bmatrix} \quad (2)$$

where a_1, a_2 are the dynamic stiffness coefficients for axial vibration and $d_1 - d_6$ are the dynamic stiffness coefficients for bending vibration. Note that two theories are provided in the appendix for axial vibration, namely, the classical theory [51] and the Rayleigh-Love theory[54]; and two theories are provided for bending vibrations, namely, the Bernoulli-Euler theory [51] and the Timoshenko theory[54,56]. For the first time, these theories have been used in all possible combinations to investigate the free vibration characteristics of multi-body systems.

2.2 Dynamic stiffness formulation for the combinations of beams and rigid bodies

The dynamic stiffness formulation for any combination of beams and rigid bodies for plane structures can be effectively carried out by considering essentially two possible cases, each requiring independent treatment. In the first case (Case-1) described in Section 2.2.1, the higher numbered node of a beam is connected to an arbitrary nodal point on a rigid body which may not necessarily be its centre of gravity (see **Fig. 2** and **Fig. 3**) whereas in the second case (Case-2) an arbitrary nodal point on a

rigid body which may not necessarily be its centre of gravity is connected to the lower numbered node of a beam (see **Fig.4** and **Fig.5**). A substantial majority of engineering applications are covered by these two cases.

2.2.1 Case-1: Dynamic stiffness formulation for beam- rigid body combinations

As shown in **Fig. 4**, nodes 1 is the mass centre of the rigid body ④ whereas the nodes 2 and 3 are the two ends of the beam member. Beam ① is rigidly connected to the rigid body ④ at node 2. The task is to develop the dynamic stiffness formulation for the combined structures of beam ① and rigid body ④ by focusing on the two nodes 3 and 1, eliminating the displacements of node 2, i.e. node 2 is condensed. This is achieved by shifting successively the force boundary conditions (BCs) and displacement BCs of the beam ① at node 2 to node 1, a standard technique used in the transfer matrix method.

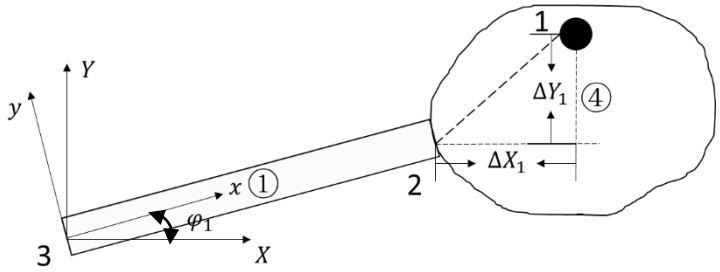

Fig. 2. Beam ① and rigid body ④ are connected at node 2.

As shown in **Fig. 4**, ΔX_1 and ΔY_1 are the relative coordinates of node 1 (mass centre of rigid body ④) with respect to node 2 of beam ① in the global coordinate system *XOY*. In order to shift the BCs of beam ① to the mass centre of the rigid body ④ directly, we first need to transfer the afore-mentioned global relative coordinates ΔX_1 and ΔY_1 into local coordinate system of the beam. Without any loss of generality, we assume the angle of the beam member (from node 3 to node 2) in the global coordinate system is φ_1. Through the coordinate system transformation, the relative coordinates Δx_1 and Δy_1 between node 1 and node 2 in the local coordinate system can be obtained by Eq.(3), and Δx_1 and Δy_1 as follows, see **Fig. 3** for details.

$$\left.\begin{aligned}\Delta x_1 &= \Delta X_1 cos\varphi_1 - \Delta Y_1 sin\varphi_1\\ \Delta y_1 &= \Delta X_1 sin\varphi_1 + \Delta Y_1 cos\varphi_1\end{aligned}\right\} \tag{3}$$

Next, the relationship of the force and displacement BCs between node 2 and node 1 can be obtained through the equilibrium and geometrical relationships, as given below in Eq. (4).

$$\left.\begin{array}{c} F_{x1} = F_{x2} \\ F_{y1} = F_{y2} \\ M_1 = M_2 - F_{y2}\Delta x_1 + F_{x2}\Delta y_1 \\ u_2 = u_1 + \theta_2 \Delta y_1 \\ w_2 = w_1 - \theta_2 \Delta x_1 \\ \theta_2 = \theta_1 \end{array}\right\} \tag{4}$$

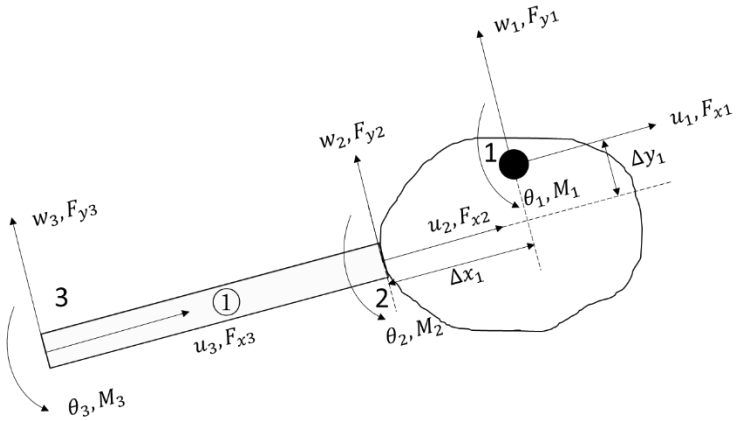

Fig. 3. Boundary conditions for displacements and forces at beam node 2 and rigid body mass centre 1 for the flexible beam-rigid body coupling member 3-1.

Eq. (4) can be rewritten in matrix form, see Eqs. (5)-(6). This is equivalent to using the force and displacement of node 2 to represent the force and displacement of node 1. We can then formulate the dynamic stiffness matrix between node 3 and node 1 through matrix operations, as shown in Eq. (7).

$$\begin{bmatrix} F_{x3} \\ F_{y3} \\ M_3 \\ F_{x1} \\ F_{y1} \\ M_1 \end{bmatrix} = \begin{bmatrix} 1 & 0 & 0 & 0 & 0 & 0 \\ 0 & 1 & 0 & 0 & 0 & 0 \\ 0 & 0 & 1 & 0 & 0 & 0 \\ 0 & 0 & 0 & 1 & 0 & 0 \\ 0 & 0 & 0 & 0 & 1 & 0 \\ 0 & 0 & 0 & \Delta y_1 & -\Delta x_1 & 1 \end{bmatrix} \begin{bmatrix} F_{x3} \\ F_{y3} \\ M_3 \\ F_{x1} \\ F_{y1} \\ M_1 \end{bmatrix} \tag{5}$$

$$\begin{bmatrix} u_3 \\ w_3 \\ \theta_3 \\ u_2 \\ w_2 \\ \theta_2 \end{bmatrix} = \begin{bmatrix} 1 & 0 & 0 & 0 & 0 & 0 \\ 0 & 1 & 0 & 0 & 0 & 0 \\ 0 & 0 & 1 & 0 & 0 & 0 \\ 0 & 0 & 0 & 1 & 0 & \Delta y_1 \\ 0 & 0 & 0 & 0 & 1 & -\Delta x_1 \\ 0 & 0 & 0 & 0 & 0 & 1 \end{bmatrix} \begin{bmatrix} u_3 \\ w_3 \\ \theta_3 \\ u_1 \\ w_1 \\ \theta_1 \end{bmatrix} \tag{6}$$

$$\begin{bmatrix} F_{x3} \\ F_{y3} \\ M_3 \\ F_{x1} \\ F_{y1} \\ M_1 \end{bmatrix} = \begin{bmatrix} 1 & 0 & 0 & 0 & 0 & 0 \\ 0 & 1 & 0 & 0 & 0 & 0 \\ 0 & 0 & 1 & 0 & 0 & 0 \\ 0 & 0 & 0 & 1 & 0 & 0 \\ 0 & 0 & 0 & 0 & 1 & 0 \\ 0 & 0 & 0 & \Delta y_1 & -\Delta x_1 & 1 \end{bmatrix} K^{①} \begin{bmatrix} 1 & 0 & 0 & 0 & 0 & 0 \\ 0 & 1 & 0 & 0 & 0 & 0 \\ 0 & 0 & 1 & 0 & 0 & 0 \\ 0 & 0 & 0 & 1 & 0 & \Delta y_1 \\ 0 & 0 & 0 & 0 & 1 & -\Delta x_1 \\ 0 & 0 & 0 & 0 & 0 & 1 \end{bmatrix} \begin{bmatrix} u_3 \\ w_3 \\ \theta_3 \\ u_1 \\ w_1 \\ \theta_1 \end{bmatrix} \tag{7}$$

where $K^{①}$ is dynamic stiffness matrix of the beam ①; which takes different formulations for different beam theories with the general form already given in Eq. (1). Thus, for the general form, Eq. (7) can be written as follow.

$$\begin{bmatrix} F_{x3} \\ F_{y3} \\ M_3 \\ F_{x1} \\ F_{y1} \\ M_1 \end{bmatrix} = \begin{bmatrix} k_{11} & k_{12} & k_{13} & k_{14} & k_{15} & k_{16}^* \\ k_{21} & k_{22} & k_{23} & k_{24} & k_{25} & k_{26}^* \\ k_{31} & k_{32} & k_{33} & k_{34} & k_{35} & k_{36}^* \\ k_{41} & k_{42} & k_{43} & k_{44} & k_{45} & k_{46}^* \\ k_{51} & k_{52} & k_{53} & k_{54} & k_{55} & k_{56}^* \\ k_{61}^* & k_{62}^* & k_{63}^* & k_{64}^* & k_{65}^* & k_{66}^* \end{bmatrix} \begin{bmatrix} u_3 \\ w_3 \\ \theta_3 \\ u_1 \\ w_1 \\ \theta_1 \end{bmatrix} \tag{8}$$

where

$$\left.\begin{array}{c} k_{16}^* = k_{16} + \Delta y_1 k_{14} - \Delta x_1 k_{15} \\ k_{26}^* = k_{26} + \Delta y_1 k_{24} - \Delta x_1 k_{25} \\ k_{36}^* = k_{36} + \Delta y_1 k_{34} - \Delta x_1 k_{35} \\ k_{46}^* = k_{46} + \Delta y_1 k_{44} - \Delta x_1 k_{45} \\ k_{56}^* = k_{56} + \Delta y_1 k_{54} - \Delta x_1 k_{55} \\ k_{66}^* = k_{66} + \Delta y_1 k_{46} - \Delta x_1 k_{56} + \Delta y_1 k_{64} + \Delta {y_1}^2 k_{44} - \Delta x_1 \Delta y_1 k_{54} - \Delta x_1 k_{65} - \Delta x_1 \Delta y_1 k_{45} + \Delta {x_1}^2 k_{55} \\ k_{61}^* = k_{61} + \Delta y_1 k_{41} - \Delta x_1 k_{51} \\ k_{62}^* = k_{62} + \Delta y_1 k_{42} - \Delta x_1 k_{52} \\ k_{63}^* = k_{63} + \Delta y_1 k_{43} - \Delta x_1 k_{53} \\ k_{64}^* = k_{64} + \Delta y_1 k_{44} - \Delta x_1 k_{54} \\ k_{65}^* = k_{65} + \Delta y_1 k_{45} - \Delta x_1 k_{55} \end{array}\right\} \tag{9}$$

In particular, for beam elements with uncoupled axial and bending vibrations in local coordinates, the dynamic stiffness of Eq. (8) takes the following form.

$$\begin{bmatrix} F_{x3} \\ F_{y3} \\ M_3 \\ F_{x1} \\ F_{y1} \\ M_1 \end{bmatrix} = \begin{bmatrix} a_1 & 0 & 0 & a_2 & 0 & \Delta y_1 a_2 \\ 0 & d_1 & d_2 & 0 & d_4 & d_5^* \\ 0 & d_2 & d_3 & 0 & -d_5 & d_6^* \\ a_2 & 0 & 0 & a_1 & 0 & \Delta y_1 a_1 \\ 0 & d_4 & -d_5 & 0 & d_1 & -d_2^* \\ \Delta y_1 a_2 & d_5^* & d_6^* & \Delta y_1 a_1 & -d_2^* & d_3^* \end{bmatrix} \begin{bmatrix} u_3 \\ w_3 \\ \theta_3 \\ u_1 \\ w_1 \\ \theta_1 \end{bmatrix} \tag{10}$$

where

$$\left.\begin{array}{c} d_5^* = d_5 - \Delta x_1 d_4 \\ d_6^* = d_6 + \Delta x_1 d_5 \\ d_2^* = d_2 + \Delta x_1 d_1 \\ d_3^* = d_3 + 2\Delta x_1 d_2 + \Delta x_1^2 d_1 + \Delta {y_1}^2 a_1 \end{array}\right\} \tag{11}$$

2.2.2 Case-2: Dynamic stiffness formulation for rigid body-beam combination

Using the same procedure as above, the dynamic stiffness formulation can be developed for the 1-5-segment of **Fig. 6**. The relative coordinates Δx_2 and Δy_2 of node 1 with respect to node 4 in the local coordinate system can be obtained through the coordinate system transformation matrix of Eq. (12) as given below.

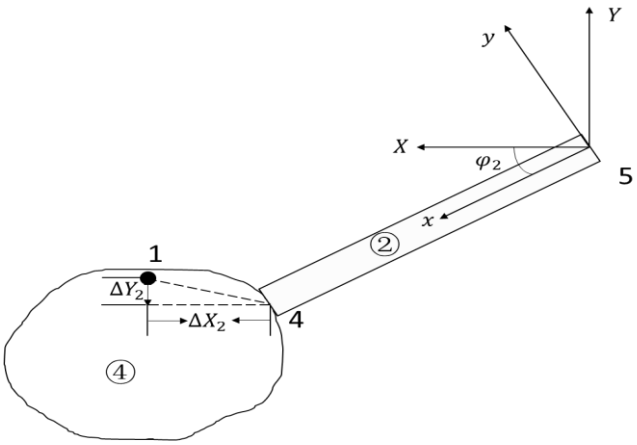

Fig.4. Rigid body ④ and beam ② are connected at node 4.

$$\left.\begin{aligned}\Delta x_2 &= \Delta X_2 cos\varphi_2 - \Delta Y_2 sin\varphi_2\\ \Delta y_2 &= \Delta X_2 sin\varphi_2 + \Delta Y_2 cos\varphi_2\end{aligned}\right\} \tag{12}$$

Next, the relationship of the force and displacement BCs between node 1 and node 4 can be obtained through the equilibrium and geometrical relationships as follows.

$$\left.\begin{aligned}F_{x1} &= F_{x4}\\ F_{y1} &= F_{y4}\\ M_1 &= M_4 + F_{y4}\Delta x_2 + F_{x4}\Delta y_2\\ u_4 &= u_1 + \theta_1 \Delta y_2\\ w_4 &= w_1 + \theta_1 \Delta x_2\\ \theta_4 &= \theta_1\end{aligned}\right\} \tag{13}$$

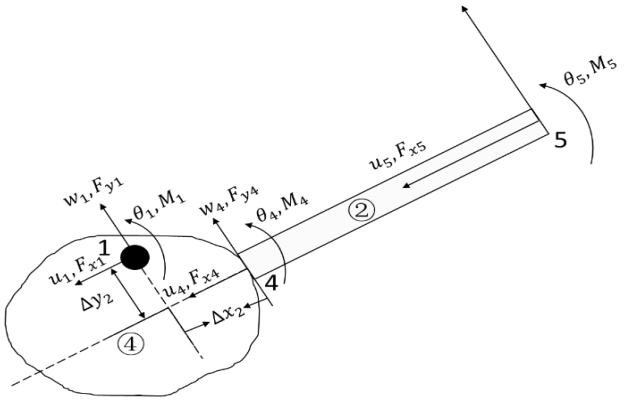

Fig.5. Boundary conditions for displacements and forces at beam node 4 and rigid body mass centre 1 for the rigid body-flexible beam coupling member 1-5.

Now, Eq. (13) can be rewritten in matrix forms, as shown in Eqs. (14)-(15). In this way, we can formulate the dynamic stiffness matrix between nodes 1 and 5 through matrix operations outlined in Eq. (16).

$$\begin{bmatrix} F_{x1} \\ F_{y1} \\ M_1 \\ F_{x5} \\ F_{y5} \\ M_5 \end{bmatrix} = \begin{bmatrix} 1 & 0 & 0 & 0 & 0 & 0 \\ 0 & 1 & 0 & 0 & 0 & 0 \\ \Delta y_2 & \Delta x_2 & 1 & 0 & 0 & 0 \\ 0 & 0 & 0 & 1 & 0 & 0 \\ 0 & 0 & 0 & 0 & 1 & 0 \\ 0 & 0 & 0 & 0 & 0 & 1 \end{bmatrix} \begin{bmatrix} F_{x4} \\ F_{y4} \\ M_4 \\ F_{x5} \\ F_{y5} \\ M_5 \end{bmatrix} \tag{14}$$

$$\begin{bmatrix} u_4 \\ w_4 \\ \theta_4 \\ u_5 \\ w_5 \\ \theta_5 \end{bmatrix} = \begin{bmatrix} 1 & 0 & \Delta y_2 & 0 & 0 & 0 \\ 0 & 1 & \Delta x_2 & 0 & 0 & 0 \\ 0 & 0 & 1 & 0 & 0 & 0 \\ 0 & 0 & 0 & 1 & 0 & 0 \\ 0 & 0 & 0 & 0 & 1 & 0 \\ 0 & 0 & 0 & 0 & 0 & 1 \end{bmatrix} \begin{bmatrix} u_1 \\ w_1 \\ \theta_1 \\ u_5 \\ w_5 \\ \theta_5 \end{bmatrix} \tag{15}$$

$$\begin{bmatrix} F_{x1} \\ F_{y1} \\ M_1 \\ F_{x5} \\ F_{y5} \\ M_5 \end{bmatrix} = \begin{bmatrix} 1 & 0 & 0 & 0 & 0 & 0 \\ 0 & 1 & 0 & 0 & 0 & 0 \\ \Delta y_2 & \Delta x_2 & 1 & 0 & 0 & 0 \\ 0 & 0 & 0 & 1 & 0 & 0 \\ 0 & 0 & 0 & 0 & 1 & 0 \\ 0 & 0 & 0 & 0 & 0 & 1 \end{bmatrix} K^{②} \begin{bmatrix} 1 & 0 & \Delta y_2 & 0 & 0 & 0 \\ 0 & 1 & \Delta x_2 & 0 & 0 & 0 \\ 0 & 0 & 1 & 0 & 0 & 0 \\ 0 & 0 & 0 & 1 & 0 & 0 \\ 0 & 0 & 0 & 0 & 1 & 0 \\ 0 & 0 & 0 & 0 & 0 & 1 \end{bmatrix} \begin{bmatrix} u_1 \\ w_1 \\ \theta_1 \\ u_1 \\ w_5 \\ \theta_5 \end{bmatrix} \tag{16}$$

where $K^{②}$ is dynamic stiffness matrix of the beam ②; which takes different formulations for different beam theories with the general form already given in Eq. (1). For the general form, Eq. (16) can be written as follows.

$$\begin{bmatrix} F_{x1} \\ F_{y1} \\ M_1 \\ F_{x4} \\ F_{y4} \\ M_4 \end{bmatrix} = \begin{bmatrix} k_{11} & k_{12} & k_{13}^* & k_{14} & k_{15} & k_{16} \\ k_{21} & k_{22} & k_{23}^* & k_{24} & k_{25} & k_{26} \\ k_{31}^* & k_{32}^* & k_{33}^* & k_{34}^* & k_{34}^* & k_{36}^* \\ k_{41} & k_{42} & k_{43}^* & k_{44} & k_{45} & k_{46} \\ k_{51} & k_{52} & k_{53}^* & k_{54} & k_{55} & k_{56} \\ k_{61} & k_{62} & k_{63}^* & k_{64} & k_{65} & k_{66} \end{bmatrix} \begin{bmatrix} u_1 \\ w_1 \\ \theta_1 \\ u_4 \\ w_4 \\ \theta_4 \end{bmatrix} \tag{17}$$

where

$$\left.\begin{array}{c} k_{13}^{*}=k_{13}+\Delta y_2 k_{11}-\Delta x_2 k_{12} \\ k_{23}^{*}=k_{23}+\Delta y_2 k_{21}-\Delta x_2 k_{22} \\ k_{33}^{*}=k_{33}+\Delta y_2 k_{13}-\Delta x_2 k_{23}+\Delta y_2 k_{31}+\Delta {y_2}^2 k_{11}-\Delta x_2 \Delta y_2 k_{21}-\Delta x_2 k_{32}-\Delta x_2 \Delta y_2 k_{12}+\Delta {x_2}^2 k_{22} \\ k_{43}^{*}=k_{43}+\Delta y_2 k_{41}-\Delta x_2 k_{42} \\ k_{53}^{*}=k_{53}+\Delta y_2 k_{51}-\Delta x_2 k_{52} \\ k_{63}^{*}=k_{63}+\Delta y_2 k_{61}-\Delta x_2 k_{62} \\ k_{31}^{*}=k_{31}+\Delta y_2 k_{11}-\Delta x_2 k_{21} \\ k_{32}^{*}=k_{32}+\Delta y_2 k_{12}-\Delta x_2 k_{22} \\ k_{34}^{*}=k_{34}+\Delta y_2 k_{14}-\Delta x_2 k_{24} \\ k_{35}^{*}=k_{35}+\Delta y_2 k_{15}-\Delta x_2 k_{25} \\ k_{36}^{*}=k_{36}+\Delta y_2 k_{16}-\Delta x_2 k_{26} \end{array}\right\} \quad (18)$$

In the case when the axial and bending vibrations of the beam element are not coupled, the above dynamic stiffness formulation takes the following degenerate form.

$$\begin{bmatrix} F_{x1} \\ F_{y1} \\ M_1 \\ F_{x5} \\ F_{y5} \\ M_5 \end{bmatrix} = \begin{bmatrix} e_1 & 0 & \Delta y_2 e_1 & e_2 & 0 & 0 \\ 0 & f_1 & f_2^{*} & 0 & f_4 & f_5 \\ \Delta y_2 e_1 & f_2^{*} & f_3^{*} & \Delta y_2 e_2 & -f_5^{*} & f_6^{*} \\ e_2 & 0 & \Delta y_2 e_2 & e_1 & 0 & 0 \\ 0 & f_4 & -f_5^{*} & 0 & f_1 & -f_2 \\ 0 & f_5 & f_6^{*} & 0 & -f_2 & f_3 \end{bmatrix} \begin{bmatrix} u_1 \\ w_1 \\ \theta_1 \\ u_5 \\ w_5 \\ \theta_5 \end{bmatrix} \quad (19)$$

where

$$\left.\begin{array}{c} f_5^{*}=f_5-\Delta x_2 f_4 \\ f_6^{*}=f_6+\Delta x_2 f_5 \\ f_2^{*}=f_2+\Delta x_2 f_1 \\ f_3^{*}=f_3+2\Delta x_2 f_2+\Delta x_2^2 f_1+\Delta {y_2}^2 e_1 \end{array}\right\} \quad (20)$$

To distinguish between different beam elements, the vectors $\boldsymbol{e}$ and $\boldsymbol{f}$ are used to represent the correlation coefficient of the axial stiffness and bending dynamic stiffness of the beam ②. Finally, we obtain the dynamic stiffness matrices of the flexible beam-rigid body coupled elements 15 and 17 according to Eqs. (19)-(20) and Eqs. (21)-(22) respectively

$$\begin{bmatrix} F_{x1} \\ F_{y1} \\ M_1 \\ F_{x7} \\ F_{y7} \\ M_7 \end{bmatrix} = \begin{bmatrix} g_1 & 0 & \Delta y_3 g_1 & g_2 & 0 & 0 \\ 0 & h_1 & h_2^{*} & 0 & h_4 & h_5 \\ \Delta y_3 g_1 & h_2^{*} & h_3^{*} & \Delta y_3 g_2 & -h_5^{*} & h_6^{*} \\ g_2 & 0 & \Delta y_3 g_2 & g_1 & 0 & 0 \\ 0 & h_4 & -h_5^{*} & 0 & h_1 & -h_2 \\ 0 & h_5 & h_6^{*} & 0 & -h_2 & h_3 \end{bmatrix} \begin{bmatrix} u_1 \\ w_1 \\ \theta_1 \\ u_7 \\ w_7 \\ \theta_7 \end{bmatrix} \quad (21)$$

where

$$\left.\begin{aligned} h_5^* &= h_5 - \Delta x_3 h_4 \\ h_6^* &= h_6 + \Delta x_3 h_5 \\ h_2^* &= h_2 + \Delta x_3 h_1 \\ h_3^* &= h_3 + 2\Delta x_3 h_2 + \Delta x_3^2 h_1 + \Delta {y_3}^2 g_1 \\ \Delta x_3 &= \Delta X_3 cos\varphi_3 - \Delta Y_3 sin\varphi_3 \\ \Delta y_3 &= \Delta X_3 sin\varphi_3 + \Delta Y_3 cos\varphi_3 \end{aligned}\right\} \tag{22}$$

and Δx_3 and Δy_3 are the relative coordinates of node 1 and node 6 in the local coordinate system, which can be obtained by the coordinate system transformation matrix. The vectors $\boldsymbol{g}$ and $\boldsymbol{h}$ are used to represent the correlation coefficient of the axial stiffness and bending dynamic stiffness of the beam ③.

2.3 Assembly procedure and the application of boundary conditions

After the dynamic stiffness formulations have been completed for all beam-rigid body coupled members and rigid body-beam coupled members, they can now be assembled to form the global dynamic stiffness matrix of the final structure. The assembly process is like that of the finite element method. The most obvious advantage of the assembly process here is that it is very simple and does not require the inverse process as commonly used in the transfer matrix method. Thus the proposed technique avoids the possibility of numerical problems such as singularity. Moreover, since in the proposed method the beam-rigid body and rigid body-beam segments take the same J_0 count of the corresponding bare beams in the Wittrick-Williams algorithm, the number of dynamic stiffness elements is much smaller than that required for the finite element method, which greatly reduces the matrix size of the overall structure. Finally, the ease of assembly in the present theory is much more apparent when compared with many existing theories used for example in a two-part beam-mass system [39–43,45,55] where the mass can only be connected between two beam members.

For the multi-body structures as shown in **Fig. 2**, we have formulated the dynamic stiffness matrices of segments 3-1 (combination of beam ① and rigid body ④), 1-5 (combination of rigid body ④ and beam ②) and 1-7 (combination of rigid body ④ and beam ③). (Defective sentence. Rewrite and reword) We express them with the simplified matrices as following Eq. (23), where $k^{①}$, $k^{②}$ and $k^{③}$ represent the dynamic stiffness matrices of segments 3-1, 1-5, and 1-7, respectively.

$$k^{①} = \begin{bmatrix} k_{33}^{①} & k_{31}^{①} \\ k_{13}^{①} & k_{11}^{①} \end{bmatrix}; k^{②} = \begin{bmatrix} k_{11}^{②} & k_{15}^{②} \\ k_{51}^{②} & k_{55}^{②} \end{bmatrix}; k^{③} = \begin{bmatrix} k_{11}^{③} & k_{17}^{③} \\ k_{71}^{③} & k_{77}^{③} \end{bmatrix} \tag{23}$$

which can be assembled directly at the mass centre 1 of the rigid body to give

$$K=\begin{bmatrix} k_{33}^{①} & k_{31}^{①} & 0 & 0 \\ k_{13}^{①} & k_{11}^{①}+k_{11}^{②}+k_{11}^{③} & k_{15}^{②} & k_{17}^{③} \\ 0 & k_{51}^{②} & k_{55}^{②} & 0 \\ 0 & k_{71}^{③} & 0 & k_{77}^{③} \end{bmatrix} \tag{24}$$

where K represents a global dynamic stiffness matrix of the above two element dynamic stiffness matrices. For a coupling system consisting of beam elements ①, ② and rigid body ④, $k_{11}^{①}+k_{11}^{②}+k_{11}^{③}$ shown in Eq. (25). Note that m and I_α here are the mass and moment of inertia of the rigid body. Thus

$$\begin{aligned} &k_{11}^{①}+k_{11}^{②}+k_{11}^{③} \\ &=\begin{bmatrix} a_1+e_1+g_1-m\omega^2 & 0 & \Delta y_1 a_1+\Delta y_2 e_1+\Delta y_3 g_1 \\ 0 & d_1+f_1+h_1-m\omega^2 & -d_2{}^*+f_2{}^*+h_2{}^* \\ \Delta y_1 a_1+\Delta y_2 e_1+\Delta y_3 g_1 & -d_2{}^*+f_2{}^*+h_2{}^* & d_3{}^*+f_3^*+h_3^*-I_\alpha\omega^2 \end{bmatrix} \end{aligned} \tag{25}$$

Of course, here we have shown only the assembly of the beam elements connecting rigid bodies. The assembly procedure of other beam members at any conventional nodes without rigid bodies can be easily performed following routine procedure [56] and is omitted here for brevity.

After assembling the overall dynamic stiffness of the final structure in global or datum coordinates, any boundary conditions can be easily applied directly just as the normal cases, and the resulting matrix can be used to perform subsequent modal or response analysis in the frequency domain.

2.4 Modal analysis by using the Wittrick-Williams algorithm

The most efficient, efficient and reliable method in the dynamic stiffness framework currently available is the application of the Wittrick-Williams (W-W) algorithm, which can be exploited to compute the natural frequencies and mode shapes of the structure. The algorithm uses the Sturm sequence property of the dynamic stiffness matrix and ensures that no natural frequencies of the structure is missed. The core content of this algorithm is as follows [68]:

$$j=j_0+s\{K_f\} \tag{26}$$

For a given trial frequency ω^*, j is the number of natural frequencies passed as ω is increased from zero to ω^*. The matrix K_f , the overall dynamic stiffness matrix of the final structure whose elements all depend on ω , is evaluated at $\omega = \omega^*$; $s\{K_f\}$ is the number of negative elements on the leading diagonal of K_f^Δ, and K_f^Δ is the upper triangular matrix obtained by applying the usual form of Gauss elimination to K_f. j_0 is the number of natural frequencies of the structure still lying between $\omega = 0$ and $\omega =$

ω^* when the displacement components to which K_f corresponds are all zeroes. It is worth emphasizing that the proposed method in this paper doesn't cause any difficulties regarding the j_0 count which often happens with other methods. The problem here is overcome due to the reason that each beam-rigid body/or rigid body-beam coupled member are treated by shifting the BCs at the connecting beam node to the mass centre of the rigid body, and the coupled members are assembled at the mass centre. The concentrated mass and rotatory inertia are also finally attached to the mass centre. Therefore, the j_0 count of each beam-rigid body/or rigid body-beam coupled member is exactly the same as the bare beam without connected to any rigid bodies. For example in Ref. [43], the rigid bodies are condensed, the j_0 count is not easy to be computed and therefore, one has to refine the mesh to make the j_0 count equal to zero which leads to unnecessary extra computational costs and possibly numerical instabilities. On the contrary, one of the merits of the present theory lies in the fact that the j_0 count already available in the literature[36,54,56] for the axial and bending vibration of beam elements can be directly used to compute the natural frequencies of the structure. This no-doubt makes the proposed theory highly efficient and accurate and importantly, easy to use.
The process of solving the mode shape of the multi-body system composed of rigid bodies and beams, is divided into two parts. First, the natural frequency computed by the W-W algorithm is substituted into the global dynamic stiffness method; by assigning a value to a proper element of the displacement vector, one can solve all other elements of the displacement vector. Next, the nodal displacements of all members can be obtained including beam members without rigid bodies and beam-rigid body coupling members. For the latter, the elemental displacement in the global coordinates will be transformed to the local coordinates, and the mode shape of the beam segments and the displacement of the mass centres of the rigid bodies can be calculated. Following an inverse process in Section 2.2, the mode shapes of the beam segments can be recovered.

It is worth emphasising that there are several works using W-W algorithm based on the dynamic stiffness models of multibody systems consisting of beams and rigid-bodies, such as Su and Banerjee [43] and Ilanko [45]. However, their work developed the dynamic stiffness models for two-part beam-mass systems, in which the associated j_0 count has not been resolved. The normal practice of applying the WW algorithm in their work need to discretise the beam sections to be small enough to ensure that the j_0 is zero. This is not convenient especially when higher natural frequencies are of interest. In comparison, the proposed method has resolved the j_0 count of all beam sections and there is no need to discretise into smaller beam elements.

3 Results

The theory presented in this paper has been implemented into a Matlab code to compute numerical results. To demonstrate the exactness, efficiency and reliability of the method, some representative examples are chosen for modal analysis. Some results are compared with those available in the literature as well as with those computed by the authors using the finite element package ANSYS. In addition, different theories are applied for both axial and bending vibrations of beam members to discuss the validities of the beam theories when combined with rigid bodies.

3.1 Validation of results for representative cases

First, we compare results computed by the proposed theory for a specially designed case (see **Fig. 6**) for which the same results can also be computed directly by using conventional beam dynamic stiffness formulation. As shown in **Fig. 6**, two beam members with ends (nodes) 1 and 4 are fixed and the other ends are rigidly connected at node 2, to which a rigid body with its mass centre at node 3 is attached. The vertical distance between the mass centre of the rigid body and node 2 is Δy. Of course, this structure can be also considered by the usual dynamic stiffness formulation of beams only by adding a mass and/or rotatory inertia eccentrically to node 2 of the two-beam assembly. The specific parameters used for the structure are as follows:

For the beam elements: Young's modulus of the beam segments: $E = 1.2 \times 10^{12} N/m^2$, beam section diameter: $D = 0.02m$, mass density: ρ =10000kg/m^3, Poisson's ratio: ν=0.3, shear correction k =1, $l_1 = 1m, l_2 = 1m$. For the rigid body: M=5kg, I_α=5 kgm^2, $\Delta x_1 = \Delta x_2 = 0m$, $\Delta y_1 = \Delta y_2 = 0.2m$.

The results computed by both the present method and those by the classical dynamic stiffness (DS) method are compared in

Table 1. The present method models the eccentrical mass (with rotatory inertia) by using the procedure described in Section 2.2; whereas in the classical DS method, the eccentrical mass and rotatory inertia are superposed directly to the common node 2 of the two-beam-assembly as shown in Fig. 8. It can be seen from Table 1 that the results from the proposed theory match exactly with those computed by the classical DS method, as expected.

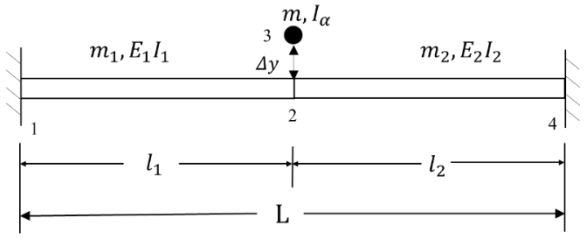

Fig. 6. A two-beam assembly connected with an eccentric rigid body.

Table 1 The first five natural frequencies of the model (*Hz*)

Mode	Present method	Normal DSM
1	19.0488	19.0488
2	27.8945	27.8945
3	195.637	195.637
4	211.017	211.017
5	535.762	535.762

Now, we adopt the example in Ref. [46] as the second example, see **Fig.7**. It is a two-part beam connected to a rigid body in the middle. The left end of the structure is fully fixed (clamped or built-in) and the right end is simply supported. The computed results are compared with those by the transfer matrix method (TMM)[46] as well as by the FEM. The data used in the analysis taken from [46] are as follows :

For the beam elements: $E = 2.069 \times 10^{11} N/m^2$, beam section diameter: $D = 0.05m$, mass density: ρ=7.8367$\times 10^3$ kg/m^3, $l_1 = 0.8m, l_2 = 1.2m$. For the rigid body: M=15.387kg, I_α=12.31 kgm^2,Δx_1=0.4m, Δx_2=0.2m, $\Delta y_1 = \Delta y_2 = 0.02m$. The first three dimensionless frequency coefficients $\lambda_i = \sqrt[4]{\frac{\omega_i \rho A L^2}{EI}} (L = l_1 + l_2 = 2m)$.

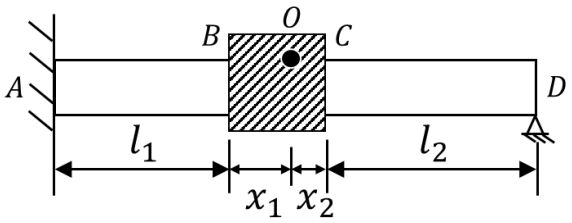

Fig.7. Elastic beam carrying a rigid body.

Table 2 Comparison on the results computed by the present method, the transfer matrix method [46] as well as the finite element method(FEM).

Mode	Present theory	TMM[46]	FEM	Rel. Err. (TMM[46] vs FEM)	Rel. Err. (present vs FEM)
1	2.40079	2.81093	2.39981	14.63%	0.04%
2	3.85796	4.68603	3.85681	17.70%	0.03%
3	5.89858	6.99522	5.89747	15.69%	0.02%

It can be clearly seen from the results in Table 2 that the theory of this paper is significantly more accurate than the transfer matrix method (TMM) of Ref. [46] when compared with the FE results using a very refined mesh. The error between the present theory and the FE results are within 0.04% whilst the error between the TMM and the FEM is larger than 14%. The reason for this is probably due to the fact that the transfer matrix method uses intensive matrix inversions one after another, which introduce numerical problems leading to errors in the results.

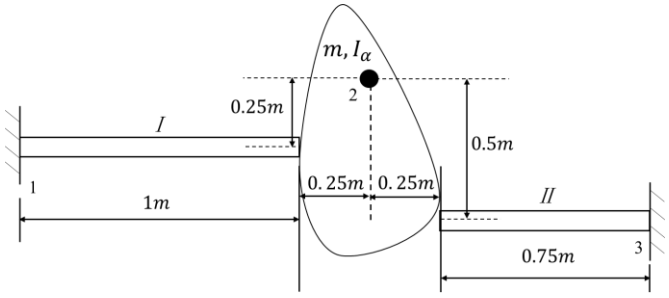

Fig. 8. A rigid body is carried by two stagger cantilevered beams.

In order to make an assessment of the accuracy of different beam theories when combined with rigid bodies, we perform the modal analysis over a very wide frequency range covering small, medium and high frequency ranges for a carefully chosen problem shown in **Fig. 8**. The specific parameters of the structure are as follows:

For beam element of type I:$EI = 6510Nm^2$,$EA = 1.25 \times 10^8 N$,ρA=4.9kg/m, ν =0.3,k=1. For beam element of type II: $EI = 2666Nm^2$, $EA = 8 \times 10^7 N$, ρA =3.14kg/m, ν =0.3, k =1. For the rigid body: M=4 kg, I_α=0.08 kgm^2,$\Delta x_1 = \Delta x_2$=0.25m, $\Delta y_1 = 0.25m$, $\Delta y_2 = 0.5m$. Coordinates of the centroid in the global coordinate system: (1.25, 0.25).

We now focus on four combinations of beam theories, two different theories for axial vibration, i.e. the classic theory and the Rayleigh-Love theory, and two different theories for bending vibration, i.e. the Bernoulli-Euler theory and the Timoshenko theory (see the appendix for details). The results are tabulated in **Table 3** where the letters 'C' and 'R' represent respectively the classical theory and Rayleigh-Love theory for axial vibration, and, the letters 'E' and 'T' represent respectively the Bernoulli-Euler theory and the Timoshenko theory for bending vibration. All results are compared with well converged FE results with fine mesh using 60, 100 and 500 elements to guarantee the accuracy provided in the results. Apart from the computation of the lower natural frequencies, higher order natural frequencies were sparingly and sparsely chosen in order to cover low, medium and high frequency range of the natural frequencies. Obviously, the higher the order of the frequency, the greater the error between the current theory and the FEM results. The computation of both DSM and FEM results in this paper was performed on a PC equipped with a 2.4 GHz Intel 4-core processor and 8 GB of memory. It's worth noting that, the computational time of both ANSYS and the proposed method arecompared by calculating all the natural frequencies of the structure within low, medium and high frequency ranges on a directly comparable basis. Therefore, the comparison is fair and convincing.

It can be found from **Table 3** that the relative error of the combination of Rayleigh-Love (axial) and Timoshenko (bending) theories is the smallest. Even for the 400th order natural frequency in the high frequency range, the largest relative error is within 4.68%. Interestingly it should be noted that the four-theory combination of results are listed with a descending order of accuracy in **Table 3**. The combination of Rayleigh-Love and Timoshenko theory gives the most accurate results, but the error progressively increases when the combination of classical-Timoshenko, Rayleigh-Love-Bernoulli-Euler and classical-Euler-Bernoulli theories are used. In terms of computational efficiency, the present DSM giving exact solutions is over 300 times faster than the commercial finite element software ANSYS which gives approximate solutions. The significantly higher computational efficiency using the DSM and the W-W algorithm arises mainly from the fact that the matrix size in the dynamic stiffness model is much smaller than the one generally encountered in the FE model. If the W-W algorithm is

applied to an FE model using $[\mathbf{K}]-\omega^2[\mathbf{M}]=0$, then the computation efficiency would not be expected to be so great.

Table 3 Comparisons of natural frequencies (*Hz*) computed by using the proposed method and the FEM.

Frequency ranges	Mode	FEM (Element Nos.)			DSM Theories（axial+bending）			
		60	100	500	CE	RE	CT	RT
Low	1	24.0371	24.0371	24.0371	24.0621 (0.10%)	24.0621 (0.10%)	24.0409 (0.02%)	24.0409 (0.02%)
	3	188.572	188.572	188.572	189.445 (0.46%)	189.445 (0.46%)	188.692 (0.06%)	188.692 (0.06%)
	5	396.096	396.101	396.131	398.821 (0.67%)	398.821 (0.67%)	396.464 (0.08%)	396.464 (0.08%)
Medium	50	17685.2	17663.3	17659.0	20687.9 (14.64%)	20665.4 (14.55%)	17898.7 (1.34%)	17882.9 (1.25%)
	100	44053.4	43954.2	43919.1	58110 (24.42%)	57426 (23.52%)	45492.4 (3.46%)	45160.6 (2.75%)
High	200	85972.1	84300.4	84146.3	151495 (44.46%)	144197 (41.64%)	88480.4 (4.90%)	88279.3 (4.68%)
	400	115660	144582	156490	363457 (56.94%)	278544 (43.82%)	162729 (3.83%)	158734 (1.41%)
Comp. Time (s)		16.48	20.32	30.31	0.09	0.09	0.10	0.09

3.2 Applications to more practical structures

We now focus on a significantly complex multi-body system to illustrate the applicability of the proposed theory to practical engineering problems. **Fig.9** shows a plane frame carrying two rigid bodies. For this problem, some selective natural frequencies covering low, mid to high frequency ranges are provided in **Table 4** and the first, third, and fifth mode shapes are shown in **Fig. 10**. Each member of the frame has the same uniform geometrical, cross sectional and material properties; Each member of the rigid body has the same mass, moment of inertia, and size in local coordinates. Then, the data used in the analysis are as follows.

For the beam elements: $EI=4\times10^6 Nm^2$, $EA=8\times10^8 N$, ρA =30*kg/m*, ν =0.3, k =1. For the two rigid body elements: M=22.5*kg*, I_α =1.875 kgm^2, $\Delta x_1=\Delta x_2$ =0.5*m*, $\Delta y_1=\Delta y_2=0.1m$. Coordinates of the centroid in the global coordinate system: I (4.5, 4.1); II (9.1, 2).

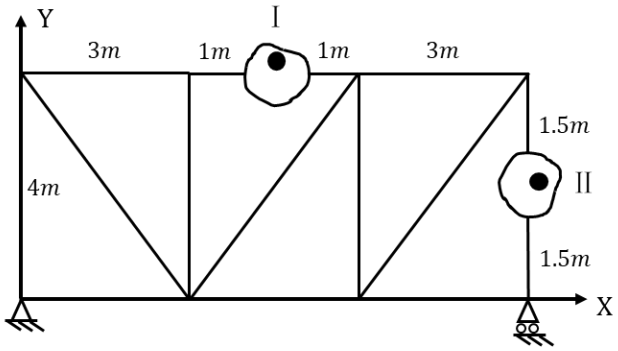

Fig.9. A plane frame carrying two rigid bodies.

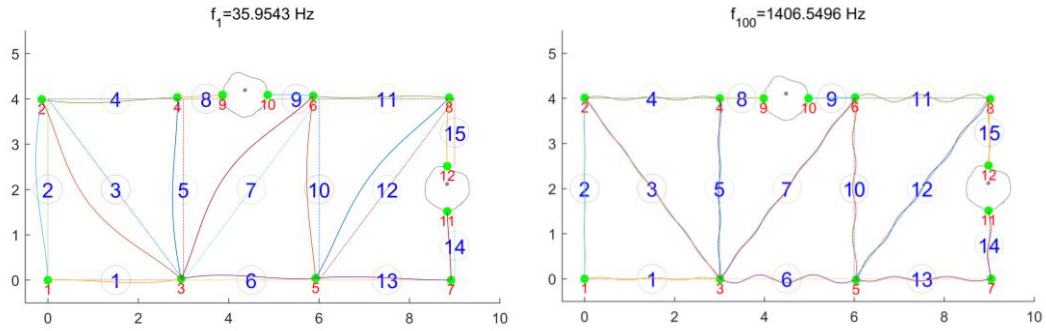

Fig. 10. The 1st and 100th mode shapes of the multi-body plane frame.

Table 4 Comparisons of natural frequencies (*Hz*) computed by using the proposed method and the FEM.

Frequency ranges	Mode	FEM (Element Nos./member)			DSM Theories（axial+bending）			
		60	100	500	CE	RE	CT	RT
Low	1	35.8961	35.8961	35.8961	36.2299 (0.92%)	36.2299 (0.92%)	35.9543 (0.16%)	35.9543 (0.16%)
	3	42.4952	42.4952	42.4952	42.9851 (1.14%)	42.9851 (1.14%)	42.5778 (0.19%)	42.5778 (0.19%)
	5	56.6970	56.6970	56.6970	57.1752 (0.84%)	57.1752 (0.84%)	56.7736 (0.13%)	56.7736 (0.13%)
Medium	50	584.902	584.902	584.902	620.786 (5.78%)	620.743 (5.77%)	589.569 (0.79%)	589.544 (0.79%)
	100	1384.71	1384.71	1384.71	1627.75 (14.93%)	1627.28 (14.91%)	1406.87 (1.58%)	1406.55 (1.55%)
High	200	3311.42	3311.01	3311.01	4298.61 (22.97%)	4284.84 (22.73%)	3413.08 (2.99%)	3412.09 (2.96%)
	400	6922.21	6920.13	6920.13	11025.8 (37.24%)	10731.4 (35.52%)	7328.47 (5.57%)	7319.63 (5.46%)
Comp. Time (s)		33.62	45.10	207.21	0.27	0.35	0.31	0.29

Based on **Table 4**, the relative error between the results for the low frequency range computed by the present theory based on Rayleigh–Love and Timoshenko theories and those by the finite element method is within 2%; and within 7% in the middle and high frequency ranges. The computational efficiency of the DSM is of course much higher than the commercial FE package ANSYS. As can be seen from **Table 4**, the DSM efficiency is as high as over 120 times of the commercial FE software package ANSYS.

The last example is shown in **Fig.11**. It is a well-thought-out problem which brings quite a lot of the efficacy and elegance of the theory. The frame in **Fig.11** has four beam elements and a rigid body element. The beam elements have two different types of beam cross sections, i.e. type I and II. The two beam members on the left are of type I whereas the two on the right are of type II. The parameters for the two types of beam cross sections.

For beam element of type I: $EI = 16Nm^2$, $EA = 4 \times 10^4 N$, ρA=1.6*kg/m*, ν=0.3, k=1. For beam element of type II: $EI = 8Nm^2$, $EA = 8 \times 10^4 N$, $\rho A = 1.4kg/m$, ν=0.3, k=1.

For the rigid body: M= 55kg, I_α=7.5kgm^2, Δx_1=0.3601m, Δx_2=0.2846m, $\Delta y_1 = -0.0171m$, $\Delta y_2 = -0.2214m$. Coordinates of the centroid in the global coordinate system: (1.5, 1.8).

The results in **Table 5** clearly shows that in the range of medium and high frequencies, the accuracy of the proposed DSM based on classical and Timoshenko theories is much better than the others. When the natural frequency is up to the 400th order, the error of the Timoshenko beam relative to the ANSYS results is only about 3.91%. The computational time of the DSM is at least two orders of magnitude lower than that of the commercial FE package ANSYS. For illustration, the first, and 100th mode shapes of the structure are shown in **Fig. 12**. It is evident that both the long- and short-wavelength modes are captured accurately by the proposed method which is normally a challenge issue for computational mechanics, see e.g., [69–71].

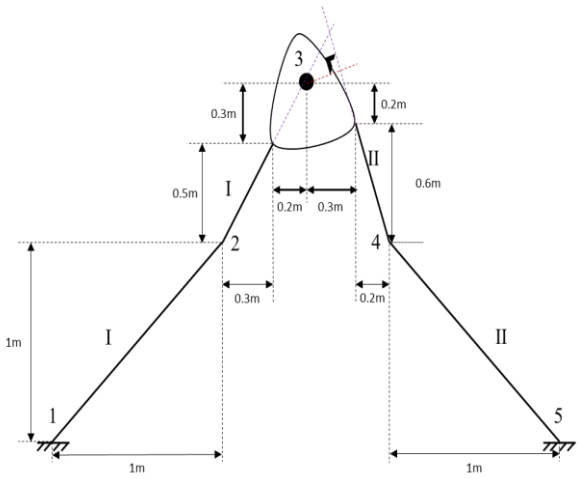

Fig.11. A rigid body is connected to two cantilevered binodal beams.

Table 5 Comparisons of natural frequencies (*Hz*) computed by using the proposed method and the FEM.

Frequency ranges	Mode	FEM (Element Nos./member)			DSM Theories（axial+bending）			
		60	100	500	CE	RE	CT	RT
Low	1	0.42105	0.42105	0.42105	0.42197 (0.22%)	0.42197 (0.22%)	0.42154 (0.12%)	0.42154 (0.12%)
	3	1.72571	1.72571	1.72571	1.73981 (0.81%)	1.73981 (0.81%)	1.72881 (0.18%)	1.72882 (0.18%)
	5	4.21682	4.21682	4.21682	4.25174 (0.82%)	4.25174 (0.82%)	4.22307 (0.15%)	4.22309 (0.15%)
Medium	50	281.431	281.391	281.381	339.106 (17.02%)	339.088 (17.02%)	290.421 (3.11%)	290.398 (3.11%)
	100	707.512	706.510	706.342	941.174 (24.95%)	933.603 (24.34%)	718.84 (1.74%)	718.610 (1.71%)
High	200	1350.90	1346.21	1346.01	2453.44 (45.14%)	2250.01 (40.18%)	1392.95 (3.37%)	1365.85 (1.45%)
	400	2128.70	2630.50	2613.12	5897.32 (55.69%)	3751.59 (30.35%)	2719.39 (3.91%)	2443.90 (6.92%)
Comp. Time (s)		22.51	45.43	85.26	0.09	0.09	0.10	0.10

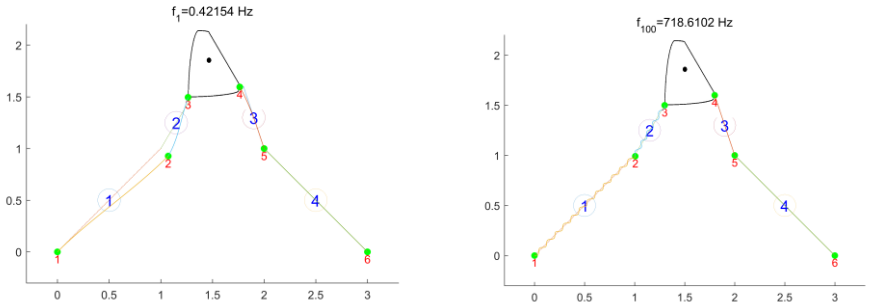

Fig. 12. The 1st and 100th mode shapes of the combined structure of rigid body and beam.

4 Conclusions

An exact dynamic stiffness formulation for a multi-body system consisting of beam and rigid body assemblies is proposed for the free vibration analysis of complex structures. The Wittrick-Williams algorithm is used as the solution technique to investigate the free vibration behaviour of complex structures consisting of multi-body systems with beams and rigid mass connected in a very general way. For beam element representation classic theory, the Rayleigh-Love theory, the Bernoulli-Euler theory and

the Timoshenko theory are used. The frequency decomposition and modal distribution are captured using several illustrative examples. The proposed theory predicts very accurately the natural frequencies in the low, medium and high frequency ranges. The theory can be further extended to complex structures in real engineering applications, so that the natural frequencies and mode shapes can be computed within any required frequency bands. The proposed theory is based on the exact solution of the governing differential equations, and it is demonstrated that the proposed theory is more accurate than the finite element solutions. Furthermore, the method is not only capable of handling more complex built-up structures than the transfer matrix method, but also is capable of computing results in a much more efficient and accurate manner due to the application of the Wittrick-Williams algorithm. This theory provides an accurate, efficient and versatile analytical method for vibration analysis and design of rigid-flexible structures. The theory is also expected to be extended to other analytical vibrational models such as membranes[72], plates [73–78], shells [79–81], solids[82] for the vibration and buckling analysis [83,84] by using associated techniques, e.g., [85–87]. Besides, the analytical nature of this proposed method facilitates the consideration of uncertainties that may occur during the manufacturing and assembly procedure, such as the uncertainties in rigid bodies (mass, rotatory inertia), the beam sections [88–90] (Young's modulus, density, cross section and etc), their connections (relative positions) and more complex engineering problems[91]. Also, in the context of inverse problems [63–65,92] for which accuracy and efficiency predictions in higher frequencies ranges are essential, the proposed method will be most useful when compared with other methods.

ACKNOWLEDGEMENTS

The authors appreciate the supports from the National Natural Science Foundation (Grant No. 11802345), State Key Laboratory of High Performance Complex Manufacturing (Grant No. ZZYJKT2019-07), the Hunan Transportation Science and Technology Foundation (Grant No. 201622) and Initial Funding of Specially-appointed Professorship (Grant No. 502045001) which made this research possible.

APPENDIX

For demonstrating purposes, we use beam element with uncoupled axial and bending vibrations. The dynamic stiffness matrix of such a beam member can be expressed as follows.

$$\begin{bmatrix} F_{x1} \\ F_{y1} \\ M_1 \\ F_{x2} \\ F_{y2} \\ M_2 \end{bmatrix} = \begin{bmatrix} a_1 & 0 & 0 & a_2 & 0 & 0 \\ 0 & d_1 & d_2 & 0 & d_4 & -d_5 \\ 0 & d_2 & d_3 & 0 & -d_5 & d_6 \\ a_2 & 0 & 0 & a_1 & 0 & 0 \\ 0 & d_4 & -d_5 & 0 & d_1 & -d_2 \\ 0 & -d_5 & d_6 & 0 & -d_2 & d_3 \end{bmatrix} \begin{bmatrix} u_1 \\ w_1 \\ \theta_1 \\ u_2 \\ w_2 \\ \theta_2 \end{bmatrix} \tag{27}$$

where a_1, a_2 are the correlation dynamic stiffness coefficients for axial vibration and

defined in Eqs.(10), (19) and (21); $d_{1\sim6}$ are the correlation dynamic stiffness coefficients for bending vibration and are defined in Eqs. (11), (20) and (22), respectively.

1 Axial vibration

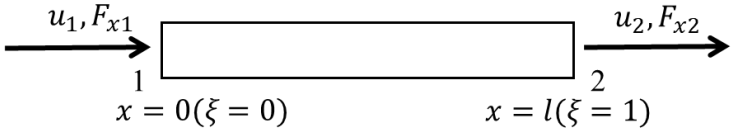

Fig. 13. Boundary conditions for displacements and forces in axial vibration.

A uniform beam of length l is shown in **Fig. 13** with the x-axis coinciding with the axis of the beam. Two theories for axial vibration are adopted in this paper, namely, Classical theory and Rayleigh-Love theory[36,54,57].

The governing differential equation (GDE) of Classical theory for free axial vibration of a beam (as shown in **Fig. 13**) is given by

$$EA\frac{\partial^2 u}{\partial x^2} - \rho A\frac{\partial^2 u}{\partial t^2} = 0 \tag{28}$$

where EA and ρA are the axial (or extensional) rigidity and mass per unit length of the beam respectively, and $u(x,t)$ is the axial displacement of the cross-section at a distance x, and t is time.

According to the derivation described in Ref. [57], the dynamic stiffness coefficient a_1 and a_2 in Eq. (27) are given as

$$a_1 = \frac{EA}{l}\mu\, cot\,\mu\,, a_2 = \frac{EA}{l}\mu\, csc\,\mu \tag{29}$$

where

$$\mu = \sqrt{\frac{\rho A\omega^2 l^2}{EA}} \tag{30}$$

The GDE of Rayleigh-Love theory for axial vibration of a beam is given as follows:

$$EA\frac{\partial^2 U}{\partial x^2} - \rho A\frac{\partial^2 U}{\partial t^2} + \rho I_P v^2\frac{\partial^4 U}{\partial x^2 \partial t^2} = 0 \tag{31}$$

where ρ is the density of the beam element material, A is the cross-sectional area of the beam element so that ρA represents the mass per unit length, I_P is the polar second moment of area so that ρI_P represents the polar mass moment of inertia per unit length, E is the Young's modulus of the beam element material so that represents

the axial or extensional rigidity, EI and EA represents the axial or extensional bending stiffness and rigidity of the beam element and ν is the Poisson's ratio of the beam element material, $U(x)$ is the amplitude of axial vibration. Based on Ref. [54], the dynamic stiffness coefficient a_1 and a_2 of Eq. (28) can be given as follows.

$$a_1 = \frac{EA}{l}\gamma(1-\beta^2)\,cot\,\gamma\,, a_2 = \frac{EA}{l}\gamma(1-\beta^2)\,csc\,\gamma \tag{32}$$

where

$$\gamma^2 = \frac{\alpha^2}{1-\beta^2}; \alpha^2 = \frac{\rho A\omega^2 l^2}{EA}; \beta^2 = \frac{\rho I_P \nu^2 \omega^2}{EA} \tag{33}$$

2 Bending vibration

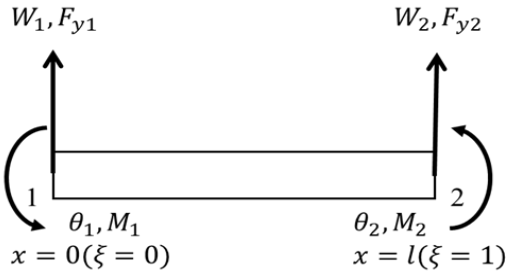

Fig.14. Boundary conditions for displacements and forces in bending (flexural) vibration

Similarly, two theories for bending vibration are adopted in this paper, namely, Euler-Bernoulli theory and Timoshenko theory[52–54,56–58].

The GDE of Euler-Bernoulli theory for bending vibration of a beam is given as follows:

$$EI\frac{\partial^4 w}{\partial x^4} + \rho A\frac{\partial^2 w}{\partial t^2} = 0 \tag{34}$$

where EI and ρA are the bending (or flexural) rigidity and mass per unit length of the beam respectively, and $w(x,t)$ is the bending (or flexural) displacement of the cross-section at a distance x and t is time.

$$\left.\begin{array}{c} d_1 = R_3\lambda^3(\sin(\lambda)\cosh(\lambda) + \cos(\lambda)\sinh(\lambda))/\delta \\ d_2 = R_2\lambda^2\sin(\lambda)\sinh(\lambda)/\delta \\ d_3 = R_1\lambda(\sin(\lambda)\cosh(\lambda) - \cos(\lambda)\sinh(\lambda))/\delta \\ d_4 = -R_3\lambda^3(\sin(\lambda) + \sinh(\lambda))/\delta \\ d_5 = R_2\lambda^2(\cosh(\lambda) - \cos(\lambda))/\delta \\ d_6 = R_1\lambda(\sinh(\lambda) - \sin(\lambda))/\delta \end{array}\right\} \tag{35}$$

where

$$R_1 = \frac{EI}{l}, \qquad R_2 = \frac{EI}{l^2}, \qquad R_3 = \frac{EI}{l^3} \tag{36}$$

$$\lambda = \sqrt[4]{\frac{m\omega^2 L^2}{EI}}, \qquad \delta = 1 - cos(\lambda)cosh(\lambda) \tag{37}$$

The GDE of Timoshenko theory for bending vibration of a beam is given as follows.

$$-\rho A \frac{\partial^2 w}{\partial t^2} + kAG \frac{\partial}{\partial x}\left(\frac{\partial w}{\partial x} - \theta\right) = 0 \tag{38}$$

$$-\rho I \frac{\partial^2 \theta}{\partial t^2} + EI \frac{\partial \theta^2}{\partial x^2} + kAG \frac{\partial}{\partial x}\left(\frac{\partial w}{\partial x} - \theta\right) = 0 \tag{39}$$

where ρ is the density of the beam element material, A is the cross-sectional area of the beam element so that ρA represents the mass per unit length, I_P is the polar second moment of area so that ρI_P represents the polar mass moment of inertia per unit length, E is the Young's modulus of the beam element material so that represents the axial or extensional rigidity, EI and EA represents the axial or extensional bending stiffness and rigidity of the beam element and ν is the Poisson's ratio of the beam element material. kAG is the shear rigidity of the beam with *k* being the shear correction (also known as the shape factor) .

The natural boundary conditions are as follows.

Shear Force: $$v = kAG\left(\frac{\partial w}{\partial x} - \theta\right) = -\rho I \frac{\partial^2 \theta}{\partial t^2} + EI \frac{\partial \theta^2}{\partial x^2} \tag{40}$$

Bending Moment: $$m = -EI \frac{\partial \theta}{\partial x} \tag{41}$$

$$\left.\begin{array}{c} d_1 = W_3 b^2 \Gamma(C\bar{S} + \eta S\bar{C})/(\Lambda\phi) \\ d_2 = W_2 Z\Gamma\{(\phi + j\eta\Lambda)S\bar{S} - (\Lambda - \eta\phi)(1 - C\bar{C})\}/(\Lambda + \eta\phi) \\ d_3 = W_1\Gamma(S\bar{C} - j\eta C\bar{S}) \\ d_4 = -W_3 b^2 \Gamma(\bar{S} + \eta S)/(\Lambda\phi) \\ d_5 = W_2 Z\Gamma(\bar{C} - C) \\ d_6 = W_1\Gamma(j\eta\bar{S} - S) \end{array}\right\} \tag{42}$$

with

$$W_1 = \frac{EI}{l}; W_2 = \frac{EI}{l^2}; W_3 = \frac{EI}{l^3} \tag{43}$$

$$b^2 = \frac{\rho A \omega^2 l^4}{EI}; r^2 = \frac{I}{Al^2}; s^2 = \frac{EI}{kAGl^2}; b^2 r^2 s^2 = \frac{\rho I \omega^2}{kAG} \tag{44}$$

$$\phi^2 = \frac{b^2(r^2+s^2)}{2} + \frac{b^2}{2}\sqrt{(r^2+s^2) + \frac{4}{b^2}(1 - b^2 r^2 s^2)} \tag{45}$$

$$\Lambda^2 = \frac{-\frac{b^2(r^2+s^2)}{2} + \frac{b^2}{2}\sqrt{(r^2+s^2) + \frac{4}{b^2}(1 - b^2 r^2 s^2)}}{j} \tag{46}$$

$$j = 1 \; for \; b^2 r^2 s^2 < 1; j = -1 \; for \; b^2 r^2 s^2 > 1 \tag{47}$$

$$\Gamma = (\Lambda + \eta\phi)/\{2\eta(1 - C\bar{C}) + (1 - j\eta^2) S\bar{S}\} \tag{48}$$

$$\left.\begin{array}{c} S = \sin\phi; C = \cos\phi \\ \bar{S} = \sinh\Lambda; \bar{C} = \cosh\Lambda \\ \bar{S} = \sin\Lambda; \bar{C} = \cos\Lambda \end{array}\right\} \tag{49}$$

$$Z = \phi - \frac{b^2 s^2}{\phi}; \eta = \frac{Z}{j\,\Lambda + \frac{b^2 s^2}{\Lambda}} \tag{50}$$

3 Mode count of fully clamped beam element for Wittrick-Williams algorithm

The j_0 count in Eq.(26) for beam based on different theories are given as follows.

For the classic theory:

$$j_0 = highest\ integer < \frac{\mu}{\pi} \tag{51}$$

For the Rayleigh–Love theory:

$$j_0 = highest\ integer < \frac{\gamma}{\pi} \tag{52}$$

For the Euler-Bernoulli theory:

$$j_0 = i - \frac{1}{2}\{1 - (-1)^i sign(\delta)\} \tag{53}$$

where *i* is the highest integer < μ/π and sign (δ) is 1 or -1 depending on the sign of δ.

For the Timoshenko theory:

$$j_0 = j_c - \left[2 - sign\{d_3\} - sign\left\{d_3 - \frac{{d_6}^2}{d_3}\right\}\right] \tag{54}$$

where sign{ } is + 1 or − 1 depending on the sign of the quantity within the curly bracket, and j_c is given by

$$\left.\begin{aligned} j_c &= j_d \ \ for\ b^2r^2s^2 < 1 \\ j_c &= j_d + j_e\ for\ b^2r^2s^2 \geq 1 \end{aligned}\right\} \tag{55}$$

with

$$\left.\begin{aligned} j_d &= highest\ integer < \frac{\phi}{\pi} \\ j_d &= highest\ integer < \frac{\Lambda}{\pi} + 1 \end{aligned}\right\} \tag{56}$$

REFERENCES

[1] Wasfy T M, Noor A K. Computational strategies for flexible multibody systems[J]. Applied Mechanics Reviews, 2003, 56(6): 553–613.

[2] Yoo W S, Kim K N, Kim H W, Sohn J H. Developments of multibody system dynamics: Computer simulations and experiments[J]. Multibody System Dynamics, 2007, 18(1): 35–58.

[3] Rui X, He B, Lu Y, Lu W, Wang G. Discrete time transfer matrix method for multibody system dynamics[J]. Multibody System Dynamics, 2005, 14(3–4): 317–344.

[4] Tadikonda S S K, Baruh H. Dynamics and control of a translating flexible beam with a prismatic joint[J]. Journal of Dynamic Systems, Measurement and Control, Transactions of the ASME, 1992, 114(3): 422–427.

[5] Ni J. Energetics and stability of translating media with an arbitrarily varying length[J]. Journal of Vibration and Acoustics, Transactions of the ASME, 2000, 122(3): 295–304.

[6] Zhu W D, Ni J, Huang J. Active control of translating media with arbitrarily varying length[J]. Journal of Vibration and Acoustics, Transactions of the ASME, 2001, 123(3): 347–358.

[7] Schiehlen W, Schiehlen W, Schiehlen W. Computational dynamics: theory and applications of multibody systems[J]. European Journal of Mechanics, A/Solids, 2006, 25(4): 566–594.

[8] Ambrósio J A C, Neto M A, Leal R P. Optimization of a complex flexible multibody systems with composite materials[J]. Multibody System Dynamics, 2007, 18(2): 117–144.

[9] Wu J J. Use of the elastic-and-rigid-combined beam element for dynamic analysis of a two-dimensional frame with arbitrarily distributed rigid beam segments[J]. Applied Mathematical Modelling, 2011, 35(3): 1240–1251.

[10] Wu J J. Free vibration analysis of a rigid bar supported by arbitrary elastic beams[J]. Applied

Mathematical Modelling, Elsevier Inc., 2014, 38(7–8): 1969–1982.

[11] Nefske D J, Sung S H. Power flow finite element analysis of dynamic systems: Basic theory and application to beams[J]. Journal of Vibration and Acoustics, Transactions of the ASME, 1989, 111(1): 94–100.

[12] Goel R P. Vibrations of a beam carrying a concentrated mass[J]. Journal of Applied Mechanics, Transactions ASME, 1973, 40(3): 821–822.

[13] Laura P A A, Pombo J L, Susemihl E A. A note on the vibrations of a clamped-free beam with a mass at the free end[J]. Journal of Sound and Vibration, 1974, 37(2): 161–168.

[14] Gürgöze M. On the eigenfrequencies of a cantilever beam with attached tip mass and a spring-mass system[J]. Journal of sound and vibration, 1996, 190: 149–162.

[15] Salarieh H, Ghorashi M. Free vibration of Timoshenko beam with finite mass rigid tip load and flexural-torsional coupling[J]. International Journal of Mechanical Sciences, 2006, 48(7): 763–779.

[16] Wang L, Chen H H, He X D. Study on modal shape of the vibration of an axially moving cantilever beam with tip mass[J]. Advanced Materials Research, 2011, 211–212: 200–204.

[17] Maiz S, Bambill D V., Rossit C A, Laura P A A. Transverse vibration of Bernoulli-Euler beams carrying point masses and taking into account their rotatory inertia: Exact solution[J]. Journal of Sound and Vibration, 2007, 303(3–5): 895–908.

[18] Erol H, Gürgöze M. Longitudinal vibrations of a double-rod system coupled by springs and dampers[J]. Journal of sound and vibration, 2004, 276(1–2): 419–430.

[19] Wittrick W H, Williams F W. A general algorithm for computing natural frequencies of elastic structures[J]. The Quarterly Journal of Mechanics and Applied Mathematics, 1971, XXIV(September 1970): 263–284.

[20] Laura P A A, Susemihl E A, Pombo J L, Luisoni L E, Gelos R. On the dynamic behaviour of structural elements carrying elastically mounted, concentrated masses[J]. Applied Acoustics, 1977, 10(2): 121–145.

[21] Dowell E H. On some general properties of combined dynamical systems[J]. Journal of Applied Mechanics, 1979, 46: 206–209.

[22] Nicholson J W, Bergman L A. Free Vibration of Combined Dynamical Systems[J]. Journal of Engineering Mechanics, 1986, 112: 1–13.

[23] Ercoli L, Laura P A A. Analytical and experimental investigation on continuous beams carrying elastically mounted masses[J]. Journal of sound and vibration, 1987, 114(3): 519–533.

[24] Larrondo H , Avalos D L P A A . Natural frequencies of a Bernoulli beam carrying an elastically mounted concentrated mass[J]. Journal of Vibration and Acoustics, 1992, 19(5)(July): 461–468.

[25] Kukla S, Posiadala B. Free Vibrations Of Beams With Elastically Mounted Masses[J]. Journal of sound and vibration, 1994, 175(4): 557–564.

[26] Cha P D. Natural frequencies of a linear elastica carrying any number of sprung masses[J]. Journal of sound and vibration, 2001, 247(1): 185–194.

[27] Inceo Ğ S, Gürgöze M, Inceoğlu S, Gürgöze M. Bending vibrations of beams coupled by several double spring-mass systems[J]. Journal of Sound and Vibration, 2001, 243(2): 370–379.

[28] Wang G Y, Zheng G T. Vibration of two beams connected by nonlinear isolators: Analytical and experimental study[J]. Nonlinear Dynamics, 2010, 62(3): 507–519.

[29] Abbas L K, Zhou Q, Rui X. Frequency Determination of Beams Coupled by a Double Spring-mass System Using Transfer Matrix Method of Linear Multibody Systems[A]. International Symposium on Knowledge Acquisition and Modeling (KAM 2015)[C]. Atlantis Press, 2015: 21–24.

[30] Rezaiee-Pajand M, Hozhabrossadati S M. Free vibration analysis of a double-beam system joined by a mass-spring device[J]. Journal of Vibration and Control, 2016, 22(13): 3004–3017.

[31] Lin H-P, Yang D. Dynamic responses of two beams connected by a spring-mass device[J]. Journal of Mechanics, 2013, 29(1): 143–155.

[32] Cha P D, Honda M. Using a characteristic force approach to determine the eigensolutions of an arbitrarily supported linear structure carrying lumped attachments[J]. Journal of Vibration and Acoustics, 2010, 132(5): 051011.

[33] Cha P D, Pierre C. Frequency analysis of a linear elastic structure carrying a chain of oscillators[J]. Journal of Engineering Mechanics, 1999, 125(5): 587–591.

[34] Farghaly S H, El-Sayed T A. Exact free vibration of multi-step Timoshenko beam system with several attachments[J]. Mechanical Systems and Signal Processing, 2016, 72–73: 525–546.

[35] Jen M U, Magrab E B. Natural frequencies and mode shapes of beams carrying a two degree-Of-Freedom spring-Mass system[J]. Journal of Vibration and Acoustics, Transactions of the ASME, 1993, 115(2): 202–209.

[36] Banerjee J R. Dynamic Stiffness Formulation and Its Application for a Combined Beam and a Two Degree-of-Freedom System[J]. Journal of Vibration and Acoustics, 2003, 125(3): 351.

[37] Cha P D. Free vibration of a uniform beam with multiple elastically mounted two-degree-of-freedom systems[J]. Journal of sound and vibration, 2007, 307(1–2): 386–392.

[38] Barry O, Oguamanam D C D, Zu J W. On the dynamic analysis of a beam carrying multiple mass-spring-mass-damper system[J]. Shock and Vibration, 2014, 2014.

[39] Kopmaz O, Telli S. On the eigenfrequencies of a two-part beam-mass system[J]. Journal of Sound and Vibration, Academic Press, 2002, 252(2): 370–384.

[40] Naguleswaran S. Comments on “On the eigenfrequencies of a two-part beam–mass system”[J]. Journal of Sound and Vibration, Academic Press, 2003, 265(4): 897–898.

[41] Banerjee J R, Sobey A J. Further investigation into eigenfrequencies of a two-part beam-mass system[J]. Journal of Sound and Vibration, 2003, 265(4): 899–908.

[42] Ilanko S. Comments on “On the eigenfrequencies of a two-part beam-mass system”[J]. Journal of Sound and Vibration, Academic Press, 2003, 265(4): 909–910.

[43] Su H, Banerjee J R. Exact natural frequencies of structures consisting of two-part beam-mass systems[J]. Structural Engineering and Mechanics, 2005, 19(5): 551–566.

[44] Naguleswaran S. Vibration of an Euler-Bernoulli stepped beam carrying a non-symmetrical rigid body at the step[J]. Journal of Sound and Vibration, 2004, 271(3–5): 1121–1132.

[45] Ilanko S. Transcendental dynamic stability functions for beams carrying rigid bodies[J]. Journal of Sound and Vibration, 2005, 279(3–5): 1195–1202.

[46] Obradović A, Šalinić S, Trifković D R, Zorić N, Stokić Z. Free vibration of structures composed of rigid bodies and elastic beam segments[J]. Journal of Sound and Vibration, Academic Press, 2015, 347: 126–138.

[47] Farghaly S H, El-Sayed T A. Exact free vibration analysis for mechanical system composed of Timoshenko beams with intermediate eccentric rigid body on elastic supports: An experimental and analytical investigation[J]. Mechanical Systems and Signal Processing, Elsevier, 2017, 82: 376–393.

[48] Wu J S, Chen C T. A continuous-mass TMM for free vibration analysis of a non-uniform beam with various boundary conditions and carrying multiple concentrated elements[J]. Journal of Sound and Vibration, 2008, 311(3–5): 1420–1430.

[49] Bestle D, Abbas L K, Rui X. Recursive eigenvalue search algorithm for transfer matrix method of linear flexible multibody systems[J]. Multibody System Dynamics, 2014, 32(4): 429–444.

[50] Radovanović N V., Zorić N D, Trišović N R, Tomović A M. Free planar vibration of structures composed of rigid bodies and elastic beam segments[J]. FME Transactions, Belgrade University, 2017, 45(1): 97–102.

[51] Koloušek V. Anwendung des Gesetzes der virtuellen Verschiebungen und des Reziprozitätssatzes in der Stabwerksdynamik[J]. Ingenieur-Archiv, 1941, 12(6): 363–370.

[52] Wang T M, Kinsman T A. Vibrations of frame structures according to the Timoshenko theory[J]. Journal of Sound and Vibration, 1971, 14(2): 215–227.

[53] Howson W P, Williams F W. Natural frequencies of frames with axially loaded Timoshenko Members[J]. Journal of sound and vibration, 1973, 26(4): 503–515.

[54] Banerjee J R, Ananthapuvirajah A. An exact dynamic stiffness matrix for a beam incorporating Rayleigh–Love and Timoshenko theories[J]. International Journal of Mechanical Sciences,

2019, 150(June 2018): 337–347.

[55] El-Sayed T A, Farghaly S H. Frequency equation using new set of fundamental solutions with application on the free vibration of Timoshenko beams with intermediate rigid or elastic span[J]. Journal of Vibration and Control, SAGE Publications Inc., 2018, 24(20): 4764–4780.

[56] Howson W P, Banerjee J R, Williams F W. Concise equations and program for exact eigensolutions of plane frames including member shear[J]. Advances in Engineering Software, 1983, 5(3): 137–141.

[57] Banerjee J R. Free vibration of beams carrying spring-mass systems − A dynamic stiffness approach[J]. Computers & Structures, 2012, 104–105: 21–26.

[58] Eisenberger M. Dynamic stiffness vibration analysis using a high-order beam model[J]. International Journal for Numerical Methods in Engineering, 2003, 57(11): 1603–1614.

[59] Xiang P, Zhang L W, Liew K M. A mesh-free computational framework for predicting vibration behaviors of microtubules in an elastic medium[J]. Composite Structures, 2016, 149: 41–53.

[60] Xiang P, Liew K M. A computational framework for transverse compression of microtubules based on a higher-order Cauchy-Born rule[J]. Computer Methods in Applied Mechanics and Engineering, 2013, 254: 14–30.

[61] Oguamanam D C D. Free vibration of beams with finite mass rigid tip load and flexural-torsional coupling[J]. International Journal of Mechanical Sciences, 2003, 45(6–7): 963–979.

[62] Lin H Y, Wang C Y. Free vibration analysis of a hybrid beam composed of multiple elastic beam segments and elastic-supported rigid bodies[J]. Journal of Marine Science and Technology, 2012, 20(5): 525–533.

[63] Yan W J, Ren W X. Circularly-symmetric complex normal ratio distribution for scalar transmissibility functions. Part I: Fundamentals[J]. Mechanical Systems and Signal Processing, 2016, 80: 58–77.

[64] Yan W J, Zhao M Y, Sun Q, Ren W X. Transmissibility-based system identification for structural health Monitoring: Fundamentals, approaches, and applications[J]. Mechanical Systems and Signal Processing, 2019, 117: 453–482.

[65] Yan W J, Chronopoulos D, Cantero-Chinchilla S, Yuen K V, Papadimitriou C. A fast Bayesian inference scheme for identification of local structural properties of layered composites based on wave and finite element-assisted metamodeling strategy and ultrasound measurements[J]. Mechanical Systems and Signal Processing, 2020, 143: 106802.

[66] Williams F W, Howson W P. Compact computation of natural frequencies and buckling loads for plane frames[J]. International Journal for Numerical Methods in Engineering, 1977, 11(7): 1067–1081.

[67] Banerjee J R, Ananthapuvirajah A. Coupled axial-bending dynamic stiffness matrix for beam

elements[J]. Computers and Structures, 2019, 215: 1–9.

[68] Sobczyk K, Wedrychowicz S, Spencer B F. Dynamics of structural system with spatial randomness[J]. International Journal of Solids and Structures, 1996, 33(11): 1651–1669.

[69] Huang Q, Liu Y, Hu H, Shao Q, Yu K, Giunta G, Belouettar S, Potier-Ferry M. A Fourier-related double scale analysis on the instability phenomena of sandwich plates[J]. Computer Methods in Applied Mechanics and Engineering, 2017, 318: 270–295.

[70] Huang Q, Xu R, Liu Y, Hu H, Giunta G, Belouettar S, Potier-Ferry M. A two-dimensional Fourier-series finite element for wrinkling analysis of thin films on compliant substrates[J]. Thin-Walled Structures, 2017, 114: 144–153.

[71] Huang W, Huang Q, Liu Y, Yang J, Hu H, Trochu F, Causse P. A Fourier based reduced model for wrinkling analysis of circular membranes[J]. Computer Methods in Applied Mechanics and Engineering, 2019, 345: 1114–1137.

[72] Liu X, Zhao X, Xie C. Exact free vibration analysis for membrane assemblies with general classical boundary conditions[J]. Journal of Sound and Vibration, 2020, 485(115484).

[73] Liu L, Li J M, Kardomateas G A. Nonlinear vibration of a composite plate to harmonic excitation with initial geometric imperfection in thermal environments[J]. Composite Structures, 2019, 209: 401–423.

[74] Li J, Zhao B, Cheng H, Kardomateas G, Liu L. Nonlinear dynamic response of a sandwich structure with flexible core in thermal environments[J]. Journal of Sandwich Structures & Materials, 2020: 1–36.

[75] Liu X, Banerjee J R. An exact spectral-dynamic stiffness method for free flexural vibration analysis of orthotropic composite plate assemblies - Part I: Theory[J]. Composite Structures, 2015, 132: 1274–1287.

[76] Liu X, Banerjee J R. An exact spectral-dynamic stiffness method for free flexural vibration analysis of orthotropic composite plate assemblies - Part II: Applications[J]. Composite Structures, 2015, 132: 1274–1287.

[77] Liu X, Banerjee J R. Free vibration analysis for plates with arbitrary boundary conditions using a novel spectral-dynamic stiffness method[J]. Computers & Structures, 2016, 164: 108–126.

[78] Liu X, Xie C, Dan H-C. Exact Free Vibration Analysis for Plate Built-Up Structures under Comprehensive Combinations of Boundary Conditions[J]. Shock and Vibration, 2020, 2020(5305692): 1–21.

[79] Liu T, Wang A, Wang Q, Qin B. Wave based method for free vibration characteristics of functionally graded cylindrical shells with arbitrary boundary conditions[J]. Thin-Walled Structures, 2020, 148: 106580.

[80] Qin B, Zhong R, Wang T, Wang Q, Xu Y, Hu Z. A unified Fourier series solution for vibration analysis of FG-CNTRC cylindrical, conical shells and annular plates with arbitrary boundary

conditions[J]. Composite Structures, 2020, 232: 111549.

[81] Qin B, Wang Q, Zhong R, Zhao X, Shuai C. A three-dimensional solution for free vibration of FGP-GPLRC cylindrical shells resting on elastic foundations: a comparative and parametric study[J]. International Journal of Mechanical Sciences, 2020, 187: 105896.

[82] Liu X, Banerjee J R. A spectral dynamic stiffness method for free vibration analysis of plane elastodynamic problems[J]. Mechanical Systems and Signal Processing, 2017, 87: 136–160.

[83] Liu X, Liu X, Xie S. A highly accurate analytical spectral flexibility formulation for buckling and wrinkling of orthotropic rectangular plates[J]. International Journal of Mechanical Sciences, 2020, 168(105311).

[84] Liu X, Liu X, Zhou W. An analytical spectral stiffness method for buckling of rectangular plates on Winkler foundation subject to general boundary conditions[J]. Applied Mathematical Modelling, 2020, 86: 36–53.

[85] Liu X, Kassem H I, Banerjee J R. An exact spectral dynamic stiffness theory for composite plate-like structures with arbitrary non-uniform elastic supports, mass attachments and coupling constraints[J]. Composite Structures, 2016, 142: 140–154.

[86] Liu X. Spectral dynamic stiffness formulation for inplane modal analysis of composite plate assemblies and prismatic solids with arbitrary classical / nonclassical boundary conditions[J]. Composite Structures, 2016, 158: 262–280.

[87] Dan H-C, Yang D, Liu X, Peng A P, Tan J W. Experimental investigation on dynamic response of asphalt pavement using SmartRock sensor under vibrating compaction loading[J]. Construction and Building Materials, 2020, 247: 118592.

[88] Adhikari S, Manohar C S. Dynamic analysis of framed structures with statistical uncertainties[J]. International Journal for Numerical Methods in Engineering, 1999, 44(8): 1157–1178.

[89] Adhikari S. Doubly spectral stochastic finite-element method for linear structural dynamics[J]. Journal of Aerospace Engineering, 2011, 24(3): 264–276.

[90] Machado M R, Adhikari S, Dos Santos J M C. Spectral element-based method for a one-dimensional damaged structure with distributed random properties[J]. Journal of the Brazilian Society of Mechanical Sciences and Engineering, 2018, 40(415): 1–16.

[91] Jiang L, Liu X, Xiang P, Zhou W. Train-bridge system dynamics analysis with uncertain parameters based on new point estimate method[J]. Engineering Structures, 2019, 199: 109454.

[92] Machado M R, Adhikari S, Santos J M C D. A spectral approach for damage quantification in stochastic dynamic systems[J]. Mechanical Systems and Signal Processing, 2017, 88(2017): 253–273.